ISSN 0280-5316
ISRN LUTFD2/TFRT--5635--SE

Modelling and Opimisation of Batch Distillation

Anna Klingberg

Department of Automatic Control
Lund Institute of Technology
January 2000

Department of Automatic Control
Lund Institute of Technology
Box 118
SE-221 00 Lund Sweden

Document name
MASTER THESIS

Date of issue
February 2000

Document Number
ISRN LUTFD2/TFRT--5635--SE

Author(s)
Anna Klingberg

Supervisor
C. Löblein, Bayer AG, C.C. Pantelides, Imp.Coll., A. Rantzer LTH

Sponsoring organisation

Title and subtitle
Modelling and Optimization of Batch Distillation. (Modellering och optimering av satsvis destillation.)

Abstract

The detailed dynamic modelling, simulation and optimisation of a batch distillation process at Bayer AG is presented. The model considers a mixture of 10 components separated in a 40 tray column.

Simulations performed in the process modelling tool gPROMS proved that the model gives a very accurate description of the process behaviour. To increase the profit of the process an optimisation of the operating procedure was performed, with the reflux ratio as the only control variable. The optimisation resulted in an increased profit, i.e. the product yield was increased while at the same time production time was decreased. Another optimisation was performed to account for the periodicity of the process, by optimising the initial conditions of the batch. These depend on the amount of fresh feed and the amount and composition of material which is recycled from the intermediate cut and mixed with the fresh feed. This optimisation also resulted in an increased profit.

Overall, gPROMS proved to be a powerful tool for solving optimisation problems of large scale models of great complexity such as the batch distillation process.

Key words

Classification system and/or index terms (if any)

Supplementary bibliographical information

ISSN and key title
0280–5316

ISBN

Language
English

Number of pages
55

Recipient's notes

Security classification

The report may be ordered from the Department of Automatic Control or borrowed through:
University Library 2, Box 3, SE-221 00 Lund, Sweden
Fax +46 46 222 44 22 E-mail ub2@ub2.lu.se

Acknowledgements

I would like to thank Professor Costas Pantelides for giving me the opportunity to come to Imperial College and learn about *gPROMS* and to be able to apply these skills in an industrially relevant context at Bayer AG.

I'm grateful to Dr Christian Löblein for arranging my stay at Bayer AG and for all the time and effort he put into this project. Without his knowledge, help and trust the results now obtained would not have been.

I would also like to thank the people at Process Systems Enterprise, PSE Ltd, for providing me with a *gPROMS* license during my stay at Bayer and especially Christian Schulz for his help solving arising problems when working on the simulation of the entire batch distillation model.

For the support in Sweden I would like to thank Professor Anders Ranzter and Professor Carl-Johan Åström, who had contacts at Imperial College.

My stay at Imperial College was financially supported by the ERASMUS program and for this I'm very thankful.

1. Introduction

1.1 Background

One of the major operations in the chemical and pharmaceutical industries is the separation of liquid mixtures into their components using distillation. The distillation can be performed as either a continuous or a batch process. Batch distillation has several advantages in many cases and it is often used in industries where high purity products are produced. In particular, it is used for purifying products or recovering solvents or valuable reactants from waste steams. Batch distillation has the advantage of being much more flexible than continuous distillation, as it has more degrees of freedom (e.g. flowrate, temperature, pressure). The flexibility makes it possible to cope with varying compositions of feed and product specifications; also completely different mixtures can be separated using the same column. This is a big advantage with today's frequently changing product specification requirements of the market (Galindez and Fredenslund [11]). Furthermore batch distillation often means simpler operation and lower capital cost than continuous distillation (Skogestad, Wittgens and Sørensen [23]).

The most obvious disadvantage of batch distillation is the high cost of energy, as it most often requires more energy than continuous distillation.

The fact that the use of batch distillation as well as the competitiveness in industry has increased during the last years (Furlonge [9]) makes it interesting to model the process and to use this model for optimisation, minimising energy requirements (which, in practice, often means minimising production time) and loss of product, always maintaining high purity requirements. Further motivation is provided by the increasingly stringent environmental regulations, which make effective control of processes vital (Barolo [1]).

1.2 Problem Statement

As batch distillation is an inherently complex dynamic process (the holdup and composition of material change with time during operation) and as the model size of batch distillation quickly grows with increasing model accuracy, number of components and number of trays (in cases of tray columns), successful optimisation relies on today's fast development of computer hardware and software.

In this work the performance of the simulation and optimisation program *gPROMS* (Process System Enterprise Ltd [20] and [21]) was evaluated on a large industrial problem by implementing and modifying in *gPROMS* a model of a batch distillation process already existing at Bayer AG. More specifically, the main objective of the project was to simulate and optimise the process, and to compare the results with the existing process as well as with the results obtained using the simulation program SPEEDUP (Aspen Technology) and the optimisation program DYNOPT (RWTH Aachen). For numerical reasons and internal memory problem of DYNOPT, it had not been possible to optimise the full large scale model of the column using that package. Instead, the model had to be reduced considerably and the optimal control profile of the batch was calculated in two parts (Gautheron [12]).

The objective using *gPROMS* on the other hand was to optimise the entire batch as a whole using the full large-scale model. The objective of the optimisation was to maximise profit, i.e. minimise process time and at the same time maximise product yield.

1.3 Outline of the Thesis

Section 2 gives an overview of the process considered. The operating procedure, the feed mixture and the design of the column are described.

The detailed model of the batch distillation is then presented in section 3 and the *gPROMS* tool used to simulate and optimise this model is briefly described in section 4. The mathematical problem that is solved in *gPROMS* and the solution techniques used by *gPROMS* for the task are further outlined in section 5.

Results from the simulations and optimisations performed are presented in sections 6 and 7 respectively.

Section 8 describes the optimisation of periodic operation and presents the results obtained.

Finally conclusions are drawn and directions for future work are given in section 9.

2. Process Description

2.1 Components

The objective of the process considered is to produce C10. More specifically, starting with a feed mixture of over 30 components with an initial concentration of C10 of about 66%, the goal is a product purity of at least 98.5% C10. An example of a gas chromatography analysis of the feed is shown in appendix A.

2.2 The Column

Both a tray and a packed column are used for the separation of the mixture described above. Because of time limitation only the tray column has been considered in this work. The tray column which is used to perform the desired separation consists of 40 trays. Each tray has about 70 bubble caps and the column is about 13.5 meters high with a diameter of 1 meter. The process is schematically described in figure 2.1.

2.3 Operation Procedure

For the purposes of this thesis, the duration of the process is normalised, with 100% corresponding to 100 hours of nominal operation. The pressure difference used to regulate the production is also normalised.

2.3.1 Reflux Ratio

The operating policy used is a piecewise *constant reflux ratio*, i.e. the reflux ratio is fixed at a pre-defined value during the different time intervals of the process. This causes the distillate composition to change during the operation, as the composition of the mixture in the reboiler changes.

The operating schedule of the reflux ratio consists of five different cuts:

1. *Light component off-cut:*
   The light components are evacuated. This takes 5 hours with the reflux ratio, R=1.

2. *Off-cut:*
   A lighter component (C4) in the mixture is removed without specification. The duration of this cut is 14 hours with reflux ratio R=5.

3. *Intermediate cut:*
   The mass fraction of C10 should reach 98.4% by the end of this phase. This is achieved by using a reflux ratio of 10 over 16 hours.

4. *Main cut:*
   The mass fraction of C10 in the product accumulator should reach at least 98.5% by the end of this phase. The reflux ratio is kept at 5 over 7 hours, and is then switched to 8 for an additional 54 hours.

5. *Heavy component off-cut:*
   The heavy components are evacuated with maximum pressure and minimum reflux ratio (R=0). This phase takes 4 hours.

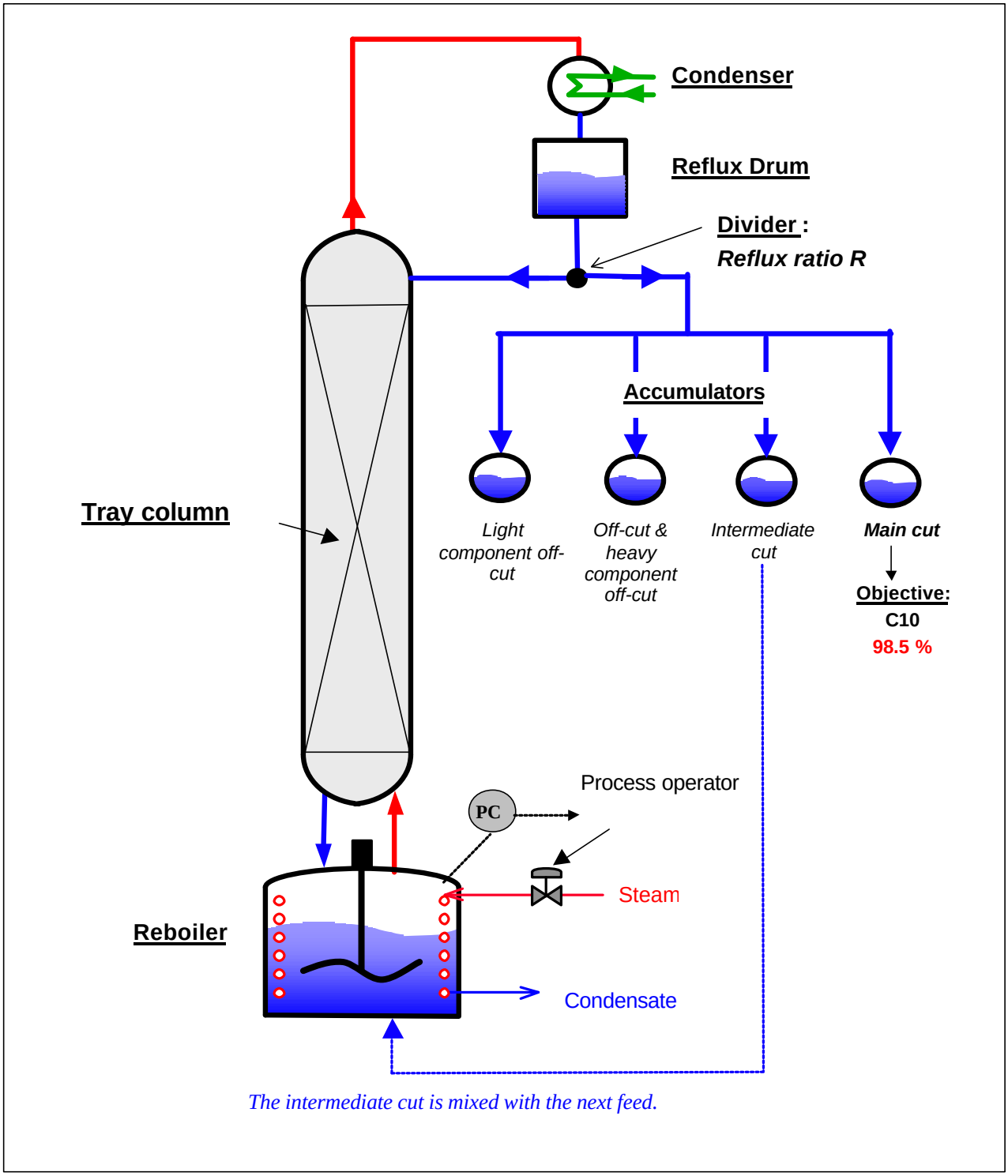

Figure 2.1 The batch distillation column.

The whole operation takes 100 hours.

2.3.2 Switching Criteria During Operation

The temperature in the column is measured during the operation. An example of a simulation of the temperature in the column is shown below (figure 2.2).

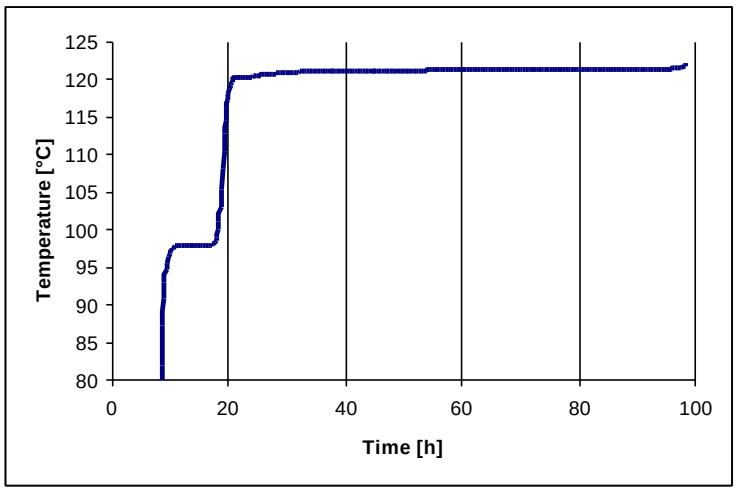

Figure 2.2 Simulation results of the temperature in the column.

The two parts with the steep gradient that can be observed in the plot tell the process operator when the off-cut and the intermediate cut begin.

A melting point analysis of the product shows the process operator when the concentration of C10 has reached the concentration constraint of 98.4% in the divider and the main cut can start. The analysis of the mixture composition could alternatively be done using gas chromatography (GC). However, the melting point analysis is much faster than a GC-analysis, taking about 5 min compared to 30 min for the GC-analysis, and the correlation between the melting point and the concentration has been proved to be good (Gautheron [12]).

When the mass fraction of C10 in the product in the accumulator used during the main cut drops below 98.5 % for a second time, the heavy component off-cut starts since the concentration of C10 in the accumulator is decreasing after this point (see figure 2.3 below).

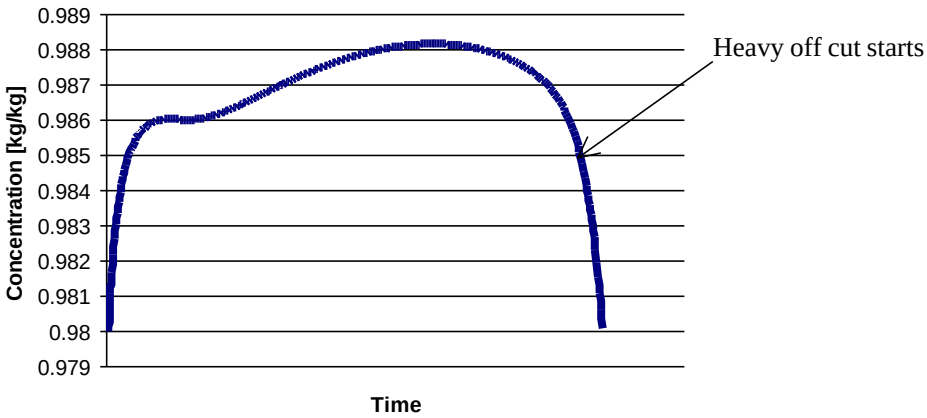

Figure 2.3 Concentration of C10 in the main cut accumulator.

2.3.2 Pressure

In addition to the reflux ratio, the pressure difference in the column (measured between reboiler and condenser) is also used as a control variable for regulating the column operation. The steam to the reboiler is controlled manually. When the pressure difference in the column is too small, the steam flow is increased by the process operator. At the top of the column, the pressure is controlled with a vacuum pump. The pressure difference in the column should measure between 0.8 and 1 bar (see table 2.1), except during the light and heavy component off-cut.

	Duration [h]	**Reflux ratio**	**Pressure difference [bar]**
Light component off-cut	5	1	-
Off-cut	16	5	0.8
Intermediate-cut	14	10	0.95
Main-cut	7	5	1
Main-cut	54	8	1
Heavy component off-cut	4	0	maximal

Table 2.1 The operating procedure.

3. The Model of the Process

3.1 Model Accuracy

In general, increased model accuracy comes at the expense of increased model complexity. and decreased computational efficiency. This means that the size of the models used in practice has to be a compromise between accuracy and simplicity to avoid numerical problem and to retain computational efficiency.

The so-called “short-cut” models for batch distillation have been very widely used in the literature. Short-cut techniques develop a direct relationship between the composition in the reboiler drum and the distillate, thus avoiding the modelling of individual trays. This leads to a significant reduction in model size. This further means that the computational effort is reduced, which was of crucial importance before today’s powerful computer hardware became available (Diwekar [7]).

Much research on batch distillation has also been done using models built up by several simplified sub models, with common assumptions such as constant liquid holdup on the tray, negligible vapour holdup, constant molal overflow (neglecting the energy balance and liquid hydraulics on each tray) and ideal equilibrium stages. Some of the assumptions can, however, cause the models to give answers far from the truth (Furlonge [10]). The usefulness of the models is reduced, potentially leading to inaccurate decisions concerning operation or design, if the knowledge of the assumptions is not good enough (Nilsson [16]).

In the case of batch distillation, the problem of model mismatch is aggravated by the “integrating” nature of the batch process. Structural or parametric errors in the model causes the error in predicted composition to increase in magnitude throughout the duration of a simulated batch run. This is fundamental to the process, and is true for any model solution technique (Bosley [4]).

With the latest computational capacity currently available at hand, it was possible to make use of a process model that is more detailed than most other models used for similar purposes.

3.2 The Structure of the Model

The model consists of seven different units:

- Tray
- Reboiler drum
- PI-controller
- Condenser
- Reflux drum
- Divider
- Accumulator

Each unit type is modelled separately. Then, one or more instances of each unit type are linked together to constitute the model of the whole process, see fig 3.1. This decomposition approach provides a better overview of the problem, greatly facilitating model development. Moreover, the constructed model is more flexible than if would be the case had it been written as a single large unit. The approach also makes it possible to make use of the already existing model library at Bayer AG.

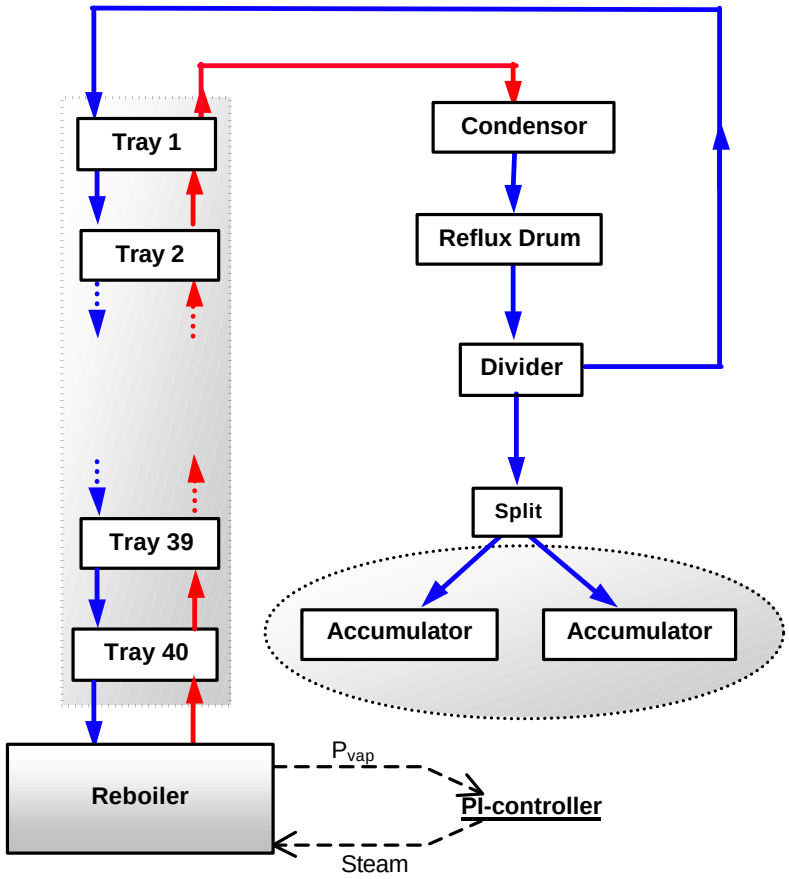

Figure 3.1 Flowsheet

The model used considers differential mass and energy balances, liquid non-ideality, and liquid hydrodynamics, with the liquid flowrate being calculated using the Francis weir formula (Perry [19]). The influence of the holdup and pressure on every tray is also taken into account. A mathematical model of each unit is described in appendix B where also a brief description of the calculations of physical properties and equilibrium relations is given.

3.3 Model Assumptions

The model for the batch distillation column has been developed using a number of model assumptions (Gautheron [12]). The final model consists of about 4200 variables/equations. The model assumptions are listed below:

1. Total condensation with no sub-cooling in the condenser.

2. No entrainment and weeping effects.

3. Constant tray efficiency.

4. Adiabatic operation.

5. Phase equilibrium.

6. Perfect mixing on the trays and in the reboiler drum.

7. Ideal vapour phase.

At the beginning of the simulation, it is assumed that the material held on the trays of the column contains only the light key component. This is more accurate than the commonly used assumption that the initial concentration in the whole column is the same as that of the feed. The latter assumption has, however, been proved to be of acceptable accuracy (Sadomoto and Miyahara [22]).

In this work, only the 10 major components of the mixture are considered as shown in table 3.1.

Component	**Mass fraction [%]**
C1	0.13
C2	0
C4	9.75
C10	66.05
C11	0.70
C12	1.35
C13	0.31
C20	15.69
C21	0.92
C28	5.10

Table 3.1 Components considered in the model.

These 10 components sum up to about 97% of the feed and the assumption has been shown to be very good (Gautheron [12]).

4. *gPROMS*

4.1 Features of *gPROMS*

gPROMS (**g**eneral **PRO**cess **M**odelling **S**ystem) process modelling software tool that is well suited for the dynamic modelling, simulation and optimisation of chemical processes. One of the reasons for this is its ability to model and handle discontinuities of the types that very often occurs in chemical processes (for example, when changing the reflux ratio during a distillation operation).

gPROMS distinguishes three fundamental types of modelling entity. `MODEL`s describe the chemical and physical behaviour of the system, defined by the equations that have been specified by the user, while `TASK`s are descriptions of the external actions and disturbances imposed on the system. Especially when dealing with batch processes, the modelling of operating procedures is of great importance. Such operating procedures are very easily described as `TASK` entities, as the *gPROMS* `TASK` language provides a large variety of features, with actions being executed in sequence or in parallel, conditionally or iteratively, thus describing the operation of the process in a very general and flexible way. The third type of entity is the `PROCESS`, which is formed by a `TASK` driving a `MODEL` with some additional information, such as initial conditions and the time variation of the input variables. Thus, a simulation is defined as the execution of such a `PROCESS`.

As with any other chemical process, the modelling of batch distillation requires the accurate consideration of physical properties in order to model the thermodynamics of the process in an accurate manner. This work has made use of the IKCAPE physical properties package for this purpose. This package has been interfaced to *gPROMS* via the *gPROMS* Foreign Object Interface (*gPROMS Introductory User Guide* [21]).

Version 1.7 of *gPROMS* was used throughout this study.

4.2 *gOPT*

Dynamic optimisation in *gPROMS* is performed by *gOPT*, which is an interface to the dynamic optimisation code DAEOPT (Vassiliadis *et al*. [24] and [25]). The *gPROMS* input file for simulation can be used in *gOPT* without any modifications. Some additional information that specifically concerns the definition of the optimisation problem has to be specified in a separate input file. This information includes the specification of the objective function and the various constraints that the optimal solution has to satisfy, the time horizon of the operation to be optimised, the control variables to be manipulated by the optimisation as well as the allowable forms of time-variation for these controls.

The user also has the option of specifying various parameters that affect the numerical performance of the optimisation. This is done by creating a parameter file which typically specifies various tolerances (relative and absolute DAE integration tolerance, steady state tolerance and optimisation tolerance) and also allows the setting of a flag that instructs *gOPT* to use a quicker but slightly less reliable method for calculating sensitivities. If no such parameter file is provided by the user, the *gOPT* solver will use default values for all of the parameters.

4.3 Limitations Using *gOPT*

The *gOPT* solver cannot handle directly discontinuities described by conditional equations (IF statements). Therefore, any conditional equation used for the simulation has to be reformulated before the simulation input file is used for optimisation.

In some cases, this can be done using the MAX operator. This is illustrated in the following example:

```
IF B + C > 0 THEN
     A = B + C
ELSE
     A = 0
```

may be reformulated as:

```
MAX(A,0) = B+C
```

Another option is to use the $(\tanh bx+1)/2$ function. As the positive parameter β grows, this function is an increasingly accurate approximation of a discontinuous unit step function:

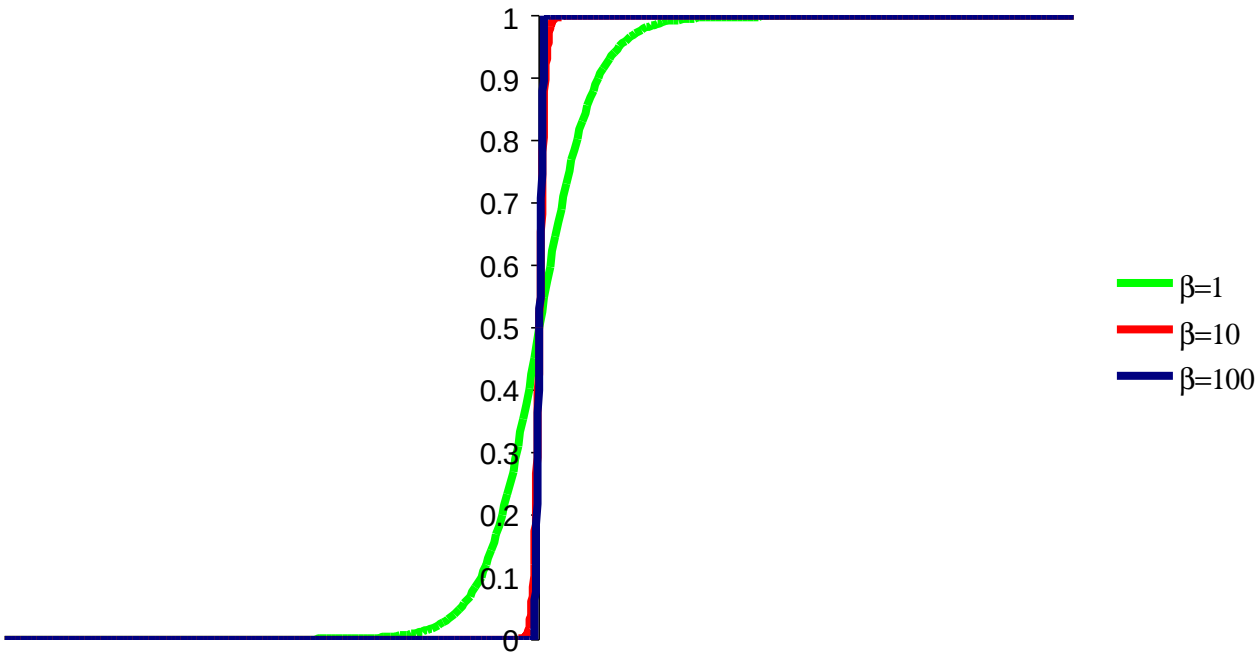

Figure 4.1 Function $y = (\tanh bx+1)/2$

An example of how to use the above function to reformulate an IF statement is shown below:

```
IF X > 0.5 THEN
     B = 2.5
ELSE
     B = 1.3
```

may be reformulated in terms of the following equations:

```
B = 2.5*A1 + 1.3*A2
A1 = (1 + tanh(β*(x-0.5)))/2
A2 = (1 - tanh(β*(x-0.5)))/2
```

Here we have introduced two new variables, A1 and A2. Note that, if x is sufficiently larger than 0.5, then A1≈1 and A2≈0; therefore, the first equation makes B ≈2.5. On the other hand, if x is sufficiently smaller than 0.5, then A1≈0 and A2≈1; and therefore B ≈1.3.

In fact, this type of reformulation may be generalised to *any* conditional equation described by an IF statement. Consider the general conditional equation:

```
IF g(x) > 0 THEN
       f1(x) = 0
ELSE
       f2(x) = 0
```

where g(x), f1(x) and f2(x) are general functions of a vector of variables x. This can be reformulated in terms of the continuous equations:

```
A1*f1(x) + A2*f2(x) = 0
A1 = (1 + tanh(β*g(x)))/2
A2 = (1 - tanh(β*g(x)))/2
```

5. The Mathematical Problem of Dynamic Optimisation

5.1 The General Form of the Dynamic Optimisation Problem

The mathematical model of a chemical process is usually described by a set of differential and algebraic equations, often abbreviated as DAEs. These equations can be written in the following way:

$$f\left(x(t), \dot{x}(t), y(t), u(t), v \right) = 0 \qquad \forall t \in \left[0, t_f\right] \qquad (5:1)$$

where $x(t)$ = differential ("state") variables

$\dot{x}(t)$ = time derivatives of the differential variables

$y(t)$ = algebraic variables

$u(t)$ = control variables

v = time invariant parameters

t_f = time horizon of interest

To solve the above equation system, initial conditions need to be given. These can be described by a set of general non-linear relations:

$$I\left(x(0), \dot{x}(t), y(0), u(0), v \right) = 0 \qquad (5:2)$$

Suitable initial conditions for optimisation of batch distillation are initial holdup, temperature and composition throughout the column (Furlonge [9]).

Optimisation in *gPROMS* aims to determine the time profile (or trajectory) of the control variables and/or the values of the time-invariant parameters which maximise or minimise a specified objective function while at the same time satisfying any imposed constraints. These constraints could be path constraints, interior point constraints or end-point constraints.

Path constraints are defined during the whole time horizon and may be written as:

$$h\left(x(t), \dot{x}(t), y(t), u(t), v, t \right) \le 0 \qquad \forall t \in \left[0, t_f\right] \qquad (5:3)$$

Interior point constraints are only defined at particular instances in time:

$$g\left(x(t_l), \dot{x}(t_l), y(t_l), u(t_l), v, t_l \right) \le 0 \qquad l = 1,2,... \qquad (5:4)$$

End-point constraints are those that must be satisfied at the final time of the operation.

For a minimisation problem, the objective function is of the general form:

$$\min \Phi\left(x(t_f), \dot{x}(t_f), y(t_f), u(t_f), v, t_f \right) \qquad (5:5)$$

5.2 Solution Techniques

The solution technique used for optimisation in *gOPT* is called control vector parameterisation (CVP). The CVP method employs a parameterisation of the control variables *u(t)*, assuming that they are described as a particular class of functions of time (for example, piecewise constant or piecewise linear functions) expressed in terms of a finite number of parameters.

At each optimisation iteration, the optimiser specifies certain values for the optimisation decision variables; the latter comprise both the parameters describing the control profiles *u(t)*, and the time-invariant parameters *v*. An integration of the DAE system can then be performed over the whole time horizon to evaluate the constraints and the objective function. The partial derivatives of these quantities with respect to the optimisation decision variables can also be evaluated during this integration if required by the optimiser.

The solution method using CVP is made as efficient as possible by adjustment of the time step and the order of integration method during each integration. The algorithm for dynamic optimisation using CVP is shown in fig 5.1 (taken from Furlonge [9]).

The repeated integration of the DAE system could be avoided by use of collocation techniques, where the state and algebraic variables are discretised as well (Logsdon and Biegler [15]) and a non-linear optimisation problem is then solved. However, this often leads to extremely large non-linear optimisation problems with thousands of equations which might be difficult to solve.

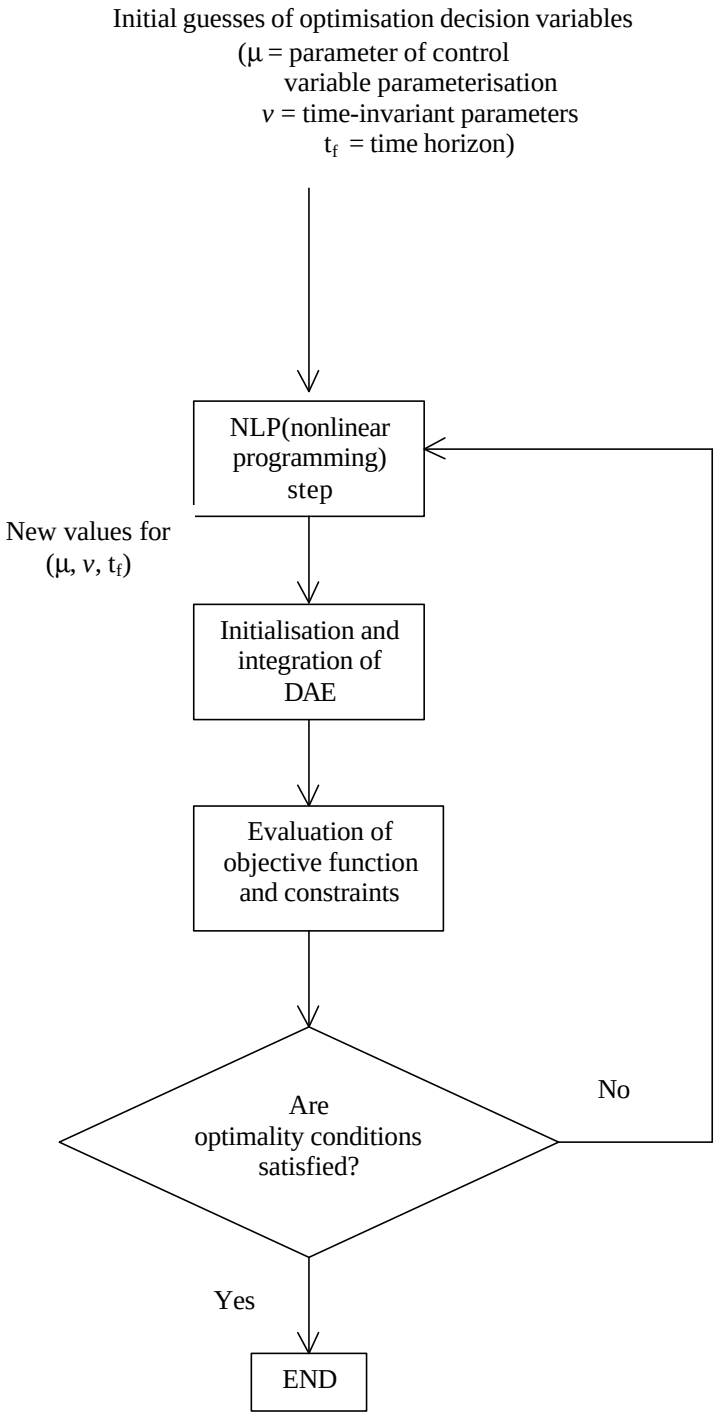

Figure 5.1 Algorithm for dynamic optimisation using CVP.

6. Simulation of the Batch Distillation Column

A simulation of the column was performed to compare the profiles with the results from the simulation performed in SPEEDUP and furthermore to evaluate the performance of *gPROMS* during simulation.

6.1 Operating Procedure

For numerical reasons, the operating procedure was slightly modified compared to the operating policy used during production (cf. section 2.3.1):

- The light off-cut, was simulated for a period 7 h instead of 5 h, with a reflux ratio of 5 instead of 1.
- The heavy component off-cut was neglected.
- The pressure difference in the column was held constant at 1 bar during the whole simulation.

Operating procedure of the simulation:

	Reflux ratio	**Duration [h]**
Light off-cut	5	7
Off-cut	5	14
Intermediate cut	10	16
Main cut	5	7
Main cut	8	54

Table 6.1 Operating procedure during simulation.

The total simulated operating time was thus 98 h.

6.2 Initialisation

For the initialisation, the column trays are assumed to contain only the light components of the mixture, whereas all the other components are charged to the reboiler. All the initial conditions given in the *gPROMS* file can be found in table 6.2.

To provide all the other variables of the equation system with reasonable initial guesses, a saved file from a former simulation was restored in the PRESET section of the *gPROMS* file.

Tray(i)	Reboiler	Accumulator 1 and 2	Accumulator 3	Accumulator 4	Reflux Drum	PI-controller
x(1) = 1.0	x(1) = 0.00066	x(1) = 1.0	x(1) = 0.01	x(1) = 0.01	$\frac{dM_i}{dt} = 0.0$	Error = 0.0
x(2) = 0.0	x(2) = 0.00147	x(2) = 0.0	x(2) = 0.0	x(2) = 0.0	$\frac{dM}{dt} = 0.0$	
x(3) = 0.0	x(3) = 0.149	x(3) = 0.0	x(3) = 0.0	x(3) = 0.0	$\frac{dU}{dt} = 0.0$	
x(4) = 0.0	x(4) = 0.663	x(4) = 0.0	x(4) = 0.06	x(4) = 0.0		
x(5) = 0.0	x(5) = 0.007031	x(5) = 0.0	x(5) = 0.91	x(5) = 0.98		
x(6) = 0.0	x(6) = 0.0136	x(6) = 0.0	x(6) = 0.03	x(6) = 0.0		
x(7) = 0.0	x(7) = 0.001	x(7) = 0.0	x(7) = 0.0	x(7) = 0.02		
x(8) = 0.0	x(8) = 0.12	x(8) = 0.0	x(8) = 0.0	x(8) = 0.0		
x(9) = 0.0	x(9) = 0.006805	x(9) = 0.0	x(9) = 0.0	x(9) = 0.0		
x(10) = 0.0	x(10) = 0.0037434	x(10) = 0.0	x(10) = 0.0	x(10) = 0.0		
$\frac{dM}{dt} = 0.0$	Level = 1.0	M = 0.01	M = 0.01	M = 0.01		
$\frac{dU}{dt} = 0.0$	$\frac{dU}{dt} = 0.0$					

Table 6.2 The initialisation conditions for simulation.

6.3 Simulation of the Simplified Model

Before the actual detailed model with 10 components and 40 trays was simulated, a simulation of a simplified model was performed. This model contains only 5 components (see table 6.3) and 20 trays. Moreover, a modified pressure drop relationship was used.

In order to make the model of the 20-tray column comparable with the actual 40-tray column, the diameter of the column and the downcomer volume were doubled.

Component	Mass fraction [%]
C1	0.13
C4	9.75
C10	66.75
C12	1.35
C20	22.02

Table 6.3 Feed composition for the simplified model.

During the simulation of the light off-cut of the simplified base case the reflux ratio was set to 3 (R = 3 was the reflux ratio used during the simulation of the light off-cut in SPEEDUP), as it did not cause any numerical problems in contrast to the simulation of the model with 10 components and 40 trays.

The composition (mass fraction) profiles obtained in the divider and the reflux ratio variation are shown below:

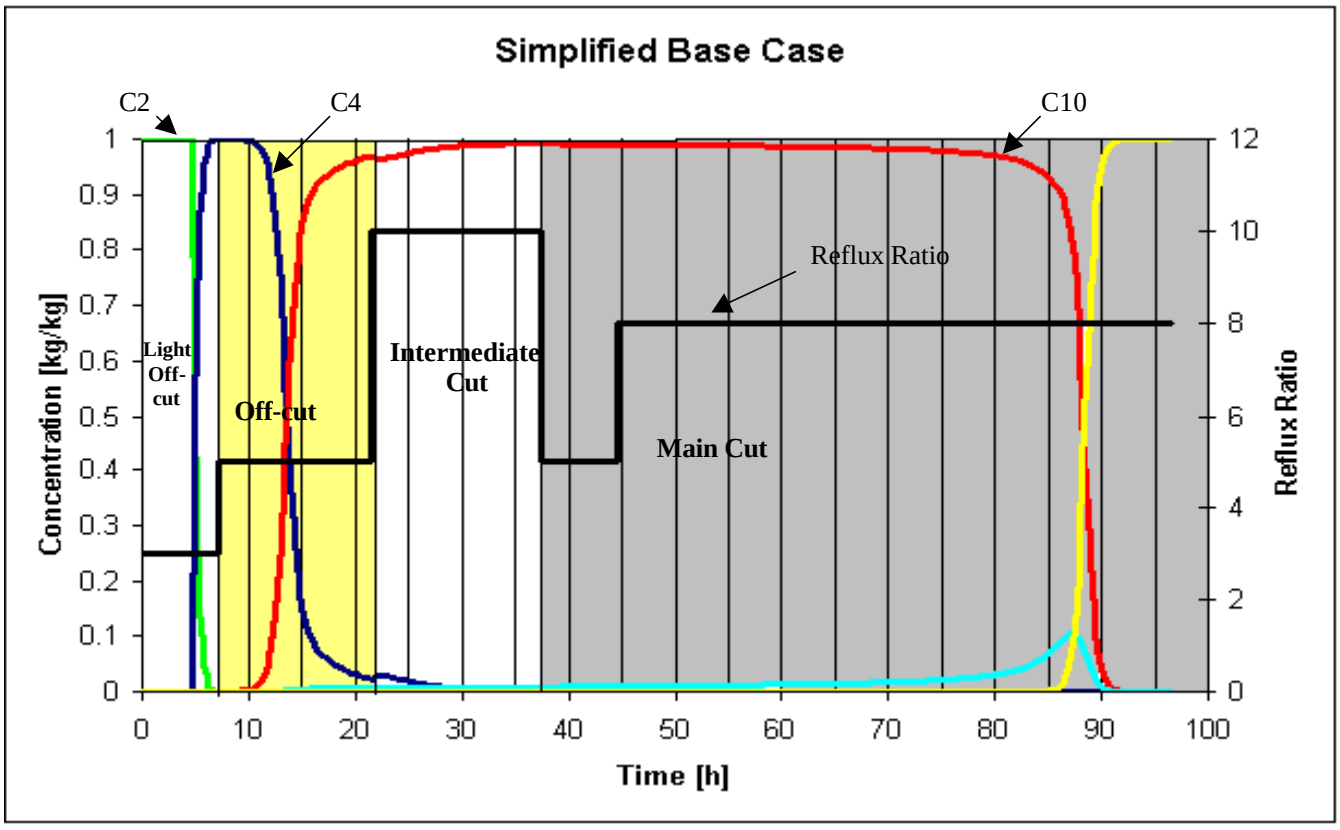

Figure 6.1 Reflux ratio and divider mass fraction profiles of simplified model at base case.

6.4 Simulation of the Detailed Model

Stability problems during the simulation of the detailed model with 10 components and 40 trays were solved by using the linear algebraic solver MA28 instead of MA48, which is the default solver in version 1.7 of gPROMS. This caused the simulation time to be even longer than if only the higher complexity of the base case model (the double amount of trays and components) had been influencing the simulation time.

The resulting mass fraction profile in the divider together with the used reflux ratio profile may be seen below:

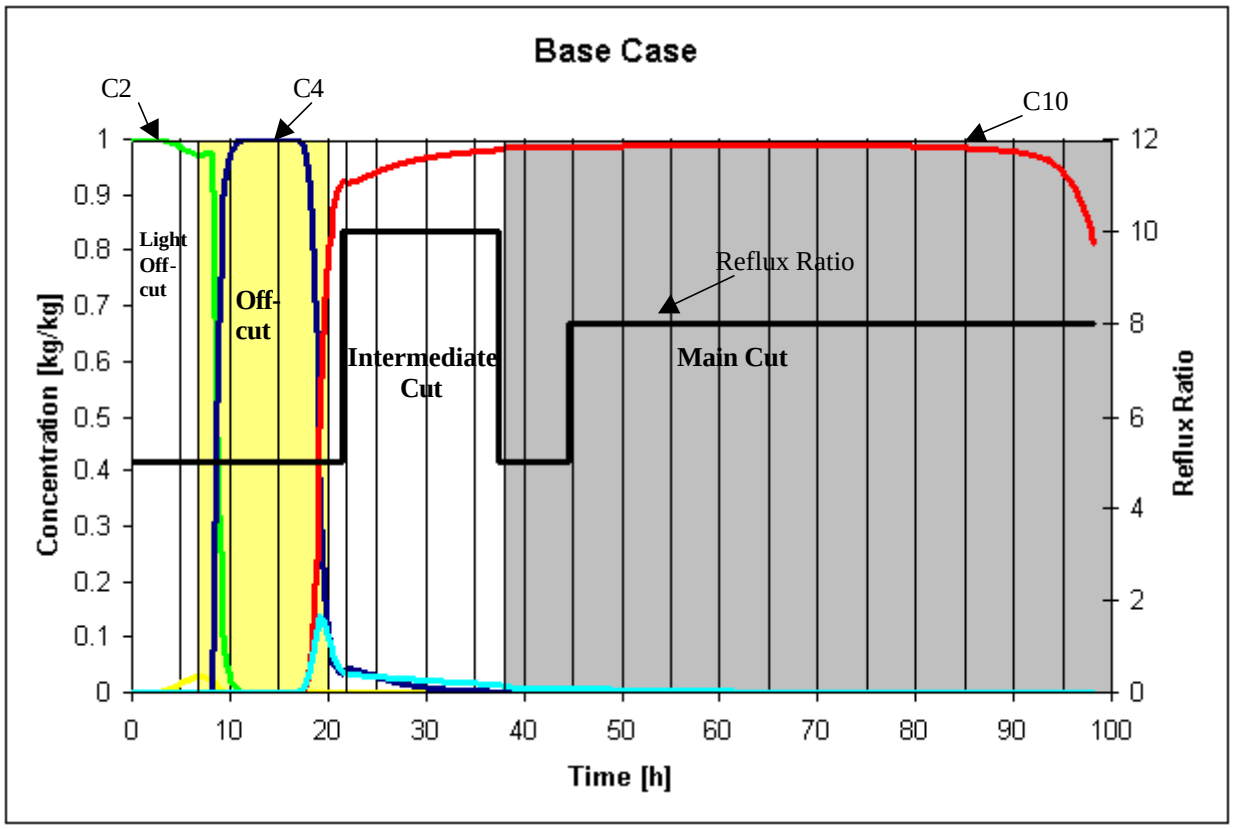

Figure 6.2 Reflux ratio and divider mass fraction profiles of detailed model at base case.

The results from the simulations agree very well with the results obtained using SPEEDUP, and they do furthermore very accurately coincide with analyses made of the operating process (Gautheron [12]).

6.5 *gPROMS* Performance

The simplified model took just over an hour to simulate on a SUN (UltraSparc Enterprise) computer and the simulation of the detailed model took about 5 hours with the same computer (see table 6.4). Considering that the model was to be used for optimisation, where this simulation calculation has to be performed several times, this is too long, for both cases.

The models were also simulated on a SGI computer, Origin 2000. The times for simulation were then reduced to just over a minute for the simplified model and about 20 minutes for the detailed model (table 6.4). For the detailed model, albeit acceptable for simulations, this is still too long for achieving reasonable optimisation time. However about 66% of this time is used only to simulate the light off-cut. It was therefore decided to omit the light off-cut from consideration during optimisation (see further section 7.).

Stability problems during the simulation were solved by using the linear algebraic solver MA28 instead of MA48, which is the default solver in version 1.7 of *gPROMS*. The drawback of using MA28 is that it uses slightly more computational time, as can be seen in table 6.4.

	SUN ULTRA (MA28)	**Origin 2000 (MA28)**	**Origin 2000 (MA48)**
Simplified model	3993 CPUs	94 CPUs	73 CPUs
Detailed model	19148 CPUs	1218 CPUs (20 min)	1099 CPUs (18 min)
Detailed model without light off-cut	Not simulated	417 CPUs (7 min)	358 CPUs (6 min)

Table 6.4 Computation times of simulation.

7. Optimisation

The objective of the optimisation was to maximise the profit, i.e. to maximise the yield of C10 and minimise production time.

The optimisation of the process using DYNOPT was only possible using the simplified model. In order to be able to make an accurate comparison of the optimisation results, ideally the optimisation should have been performed using both models. However since the objective of this work was to consider the optimisation of the entire batch of the detailed model as a benchmark for the evaluation of the performance of *gPROMS*/*gOPT*, only the detailed model was optimised.

As already mentioned, the time for simulation of the whole batch was too long to achieve reasonable optimisation times. Therefore the light off-cut was not considered, which reduces the simulation time by about 66%. The heavy component off-cut was not considered, as it is already performed in the quickest way possible, i.e. maximal steam pressure to the reboiler and no reflux. Both of these simplifications were made when optimising in DYNOPT as well.

The optimisation was first performed in two steps, like it had been done using DYNOPT. The first step was to optimise the off-cut and the intermediate cut. The column was then initialised with the state variables at the end of the intermediate cut, and the main cut was optimised over the remaining time horizon. After the two parts had been optimised separately, the operation was also optimised in a single run. The only control variable during the optimisations was the reflux ratio. The base case profile of the reflux ratio was always used as the initial guess.

7.1 Off-cut and Intermediate Cut Optimisation

The off-cut and the intermediate cut were optimised with the objective of *minimising* the loss of C10 and the production time. At the end of the intermediate cut, the mass fraction of C10 from the divider has to exceed 98.4%; this was the only endpoint-constraint imposed on the optimisation.

The objective function to be minimised was formulated as:

$$\text{Cost} = t_{prod}/t^{*}_{prod} + M_{C10}/\ M^{*}_{C10} \qquad (7:1)$$

where:

t_{prod} = production time [h]

t^{*}_{prod} = production time before optimisation = 30 [h]

M_{C10} = C10 in intermediate cut [kg]

M^{*}_{C10} = C10 in intermediate cut at base case = 1333 [kg]

The computation time used for optimisation was 11064 CPUs (about 3 h) using 13 optimisation iterations to find the optimum.

The optimal profile with 6 different intervals of reflux ratios results in a new production time of 21 h, which compared with the 30 h used in the base case, represents an improvement of

30%. The loss of product in the intermediate cut was also reduced. At optimum, the loss is 446 kg compared with 1333 kg during the base case, i.e. a reduction of product loss by 66.5%.

The resulting mass fraction profile in the divider together with the optimal reflux ratio profile are shown in figure 7.1.

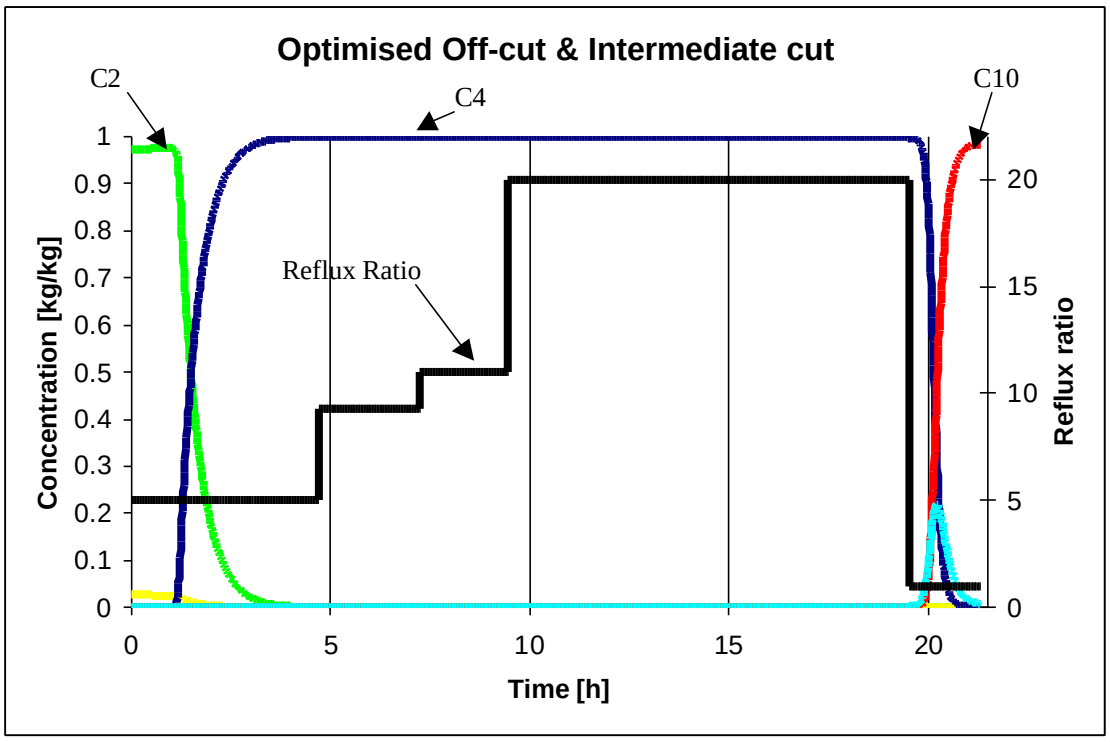

Figure 7.1 Reflux ratio and divider mass fraction profiles at optimum for off-cut and intermediate cut.

7.2 Main Cut

The objective of the optimisation of the main cut was to *maximise* the yield of product at the same time as *minimising* production time. At the end of the main cut, the mass fraction of C10 should reach over 98.5% in the main cut accumulator. This was the only endpoint-constraint that was imposed on the optimisation.

The objective function to minimise was formulated as:

$$\text{Cost} = t_{prod} - k \cdot M_{C10} \qquad (7:2)$$

where:

t_{prod} = production time [h]

M_{C10} = C10 in main cut [kmol]

k = 1.5

The parameter k is used to weight the influence of C10 produced compared to that of t_{prod}. By performing different optimisations, the most appropriate value of k was found to be 1.5. This gives a reasonable production time while the product yield is also improved.

The new production time for the main cut was 55 h, which represents an improvement of 5% over the production time of 58 h for the base case. The yield of product was improved by 6.5%, from 5368 kg to 5714 kg.

The number of control intervals used was 7, and the optimisation took 5606 CPUs (just over 1.5 h), using 13 optimisation iterations. The reason why this optimisation run only uses about half of the time used for optimising the off-cut and intermediate cut, is that the variations of the variables are much smaller, less happens in the column and the integrator can therefore take larger steps. This makes it possible to use the MA48 solver, which as shown by our simulation results, is faster than the MA28 solver that was used for the optimisation of the off-cut and intermediate cut.

The resulting mass fraction profile in the divider together with the reflux ratio profile are shown in figure 7.2.

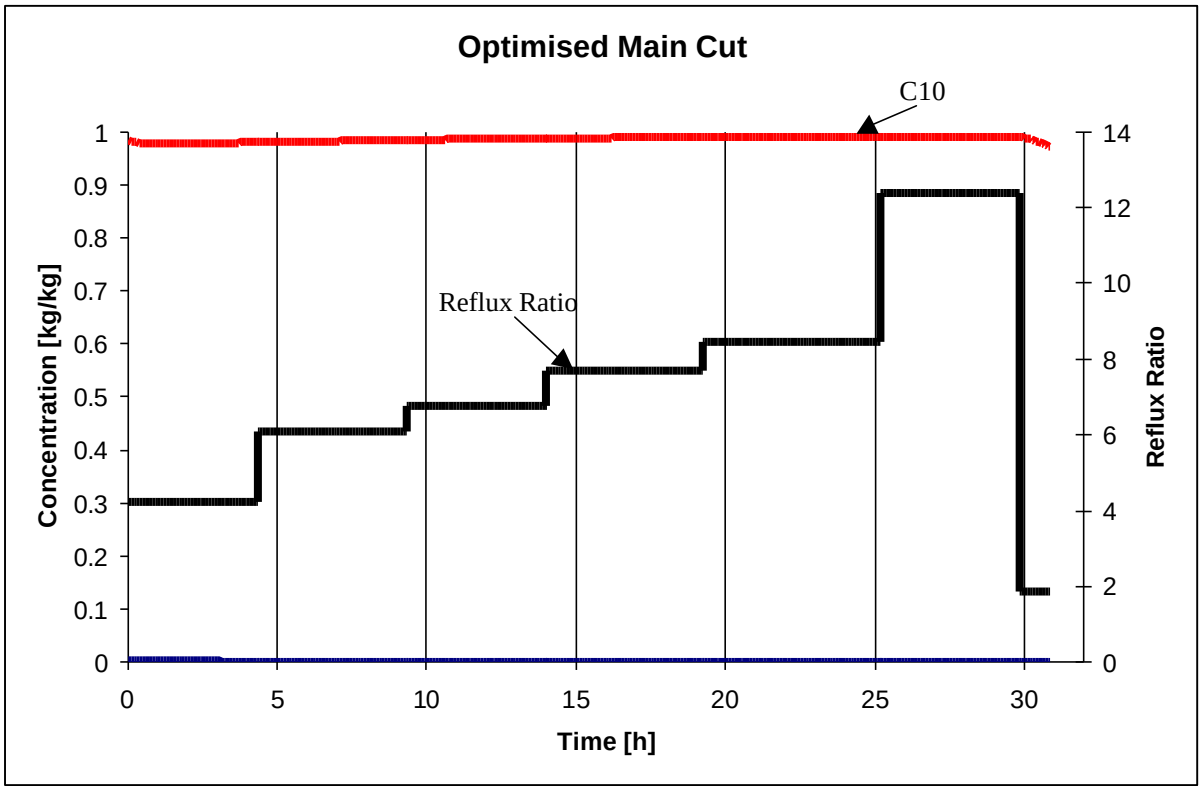

Figure 7.2 Reflux ratio and divider mass fraction profiles at optimum for main cut.

The optimisation results agree quite closely with results obtained using DYNOPT with the simplified model (Gautheron [12]). Differences can be explained by the different model complexities.

7.3 Optimisation of the Operating Procedure of the Entire Batch

Before the operating procedure of the entire batch could be optimised, the problem of switching from the intermediate cut to the main cut without using any IF statements in the model had to be solved. The solution of the problem was to use a tanh function, as described in section 4.2. Since *gPROMS* cannot currently handle excessively large values of the

the argument of the tanh function, a max and a min function additionally had to be used to limit this argument to the range [-100,+100], as shown below:

$$y = \tanh(\min(100,\max(-100,\beta*(0.5- x))))/2 \quad (7:3)$$

The model used for this optimisation employs a single accumulator used to collect the main cut. We recall that the main cut starts when the mass fraction of C10 in the divider exceeds 98.4%. At this point, the divider flow is switched to the main cut accumulator and the main cut accumulator starts to fill up. The main cut continues until the mass fraction of C10 in the accumulator reaches 98.5% for a second time (i.e. the concentration of C10 in the accumulator is decreasing) independent of the concentration of C10 in the divider. This behaviour was achieved by use of an additional tanh function and a max function, that controls the liquid flow to the accumulator. The flow is multiplied by 0 before the main cut and by 1 as soon as the mass fraction of C10 from the divider exceeds 98.4% and the main cut has started.

The number of control intervals for the reflux ratio was set to 13, which is equal to the sum of intervals during the two separate optimisations of the off-cut and intermediate cut and the main cut.

Because of the same stability problems during the off-cut and the intermediate cut as before, the MA28 solver had to be used during the optimisation. The objective function to be minimised was the same as during the optimisation of the main cut (see equation 7:2).

The results from the optimisation of the entire batch of the detailed model are not very different from the two separate optimisations. The yield of product was 5814 kg, which is an improvement of 8.3% compared to the 5368 kg achieved at base case, and 1.8% more than what was achieved when the main cut was considered separately. The new operating time obtained was 75 h, 15 % shorter than for the base case (88 h), and 1 hour less than for the combined production time of the two separate optimisations. The better results of the optimisation of the entire batch compared to the two separate optimisations are explained by the larger number of degrees of freedom when the entire batch is optimised (e.g. the number of intervals during the off-cut and intermediate cut are not fixed during the optimisation of the entire batch). The larger number of degrees of freedom also explains the longer computational time required by the optimisation: 40.9 h performing 85 optimisation iterations.

The resulting profile of divider mass fraction and reflux ratio at the optimum are shown in figure 7.3.

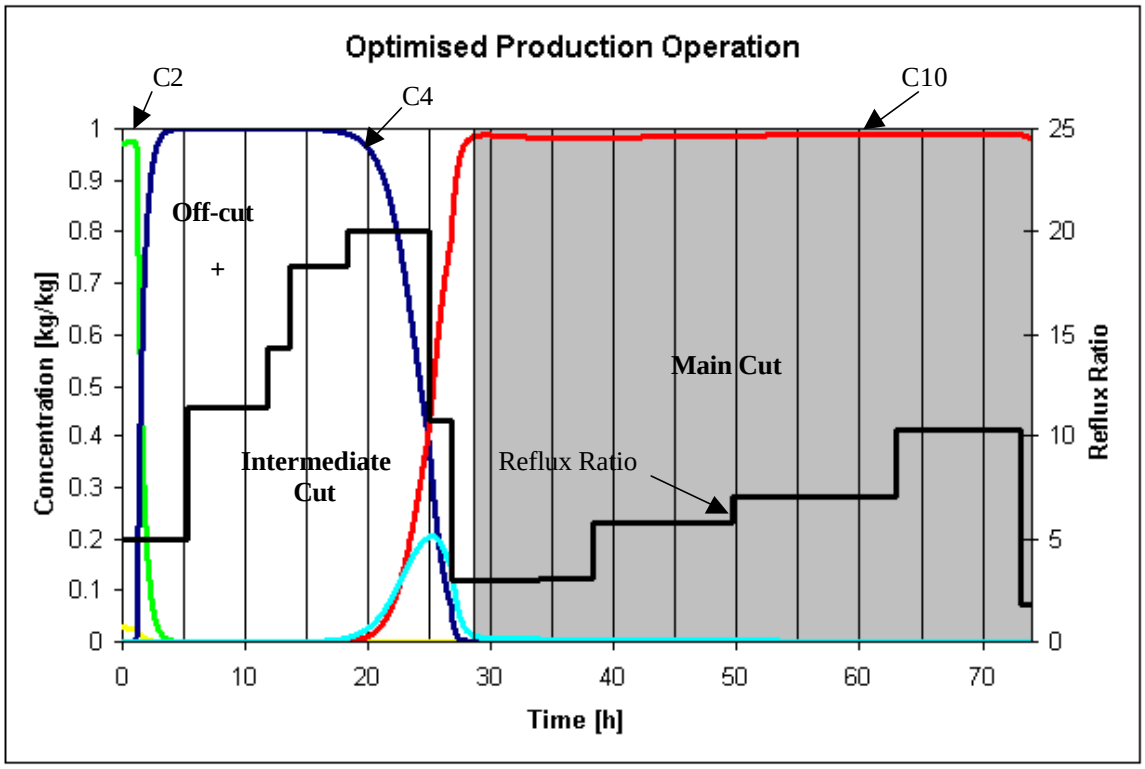

Figure 7.3 Reflux ratio and divider mass fraction profiles at optimum for the entire batch.

7.4 Summarised Results

Summarised results compared with base case:

	Off-cut & Intermediate cut		Main cut		Entire batch	
Batch time	21 h	-30%	55 h	-5%	75 h	-15%
Product yield	446 kg	-66.5%	5714 kg	+6.5%	5814 kg	+8.3%

Table 7.1 Summarised results of the optimisations.

gPROMS performance during optimisation:

	Off-cut & Intermediate cut	Main cut	Entire batch
CPU time of optimisation	11064 sec (3.1 h)	5056 sec (1.6 h)	147337 sec (40.9 h)
Number of optimisation iterations	13	13	85
Linear Algebraic Solver	MA28	MA48	MA28
Intervals of control variable optimised	6	7	13

Table 7.2 Summarised results of gPROMS performance during optimisation

A more detailed account of the *gOPT* settings and the *gPROMS* performance during the optimisations may be found in appendix C.

8. Periodic Operation

In practical operation, the contents of the accumulator used during the intermediate cut are mixed with the fresh feed for the next distillation batch and is then charged to the reboiler drum (see figure 2.1). This implies that the composition and amount of mixture obtained during the intermediate cut will influence the next batch run and its operating procedure. To take this effect into account, a periodic optimisation has to be performed considering the whole operating procedure as well as the set up time between every batch run.

8.1 Optimisation with a Multiplexer

For the optimisation of the periodic operation, a separate accumulator is needed for each cut. This can be achieved by using a *multiplexer*. The multiplexer determines the flow received by the accumulator for each of the three different cuts according to the following formulae:

Accumulator 1 : Liquid stream from divider*(*Acc*-2)*(*Acc*-3)/2
Accumulator 2 : Liquid stream from divider*(*Acc*-1)*(*Acc*-3)/(-1)
Accumulator 3 : Liquid stream from divider*(*Acc*-2)*(*Acc*-1)/2

The multiplexer adjusts the value of the control variable *Acc*. During the off-cut, *Acc* is kept at the value 1; it can be verified that, in this case, only accumulator 1 receives a non-zero flow from the divider. When the intermediate cut starts, the value of *Acc* is set to 2, and liquid only flows into accumulator 2. Finally, during the main cut *Acc* has the value of 3 and all product will be gathered in accumulator 3. The values of *Acc* are set in the *gOPT*-file used for optimisation, which means that the number of intervals during each cut has to be fixed with this method.

The use of a multiplexer also provides an alternative way of switching from the intermediate cut to the main cut. The constraint that the mass fraction of C10 has to exceed 98.4% in the divider at the start of the main cut can be imposed as an interior point constraint at the beginning of the first interval of the main cut in the *gOPT*-file instead of using a tanh function (cf. section 7.3).

Except for using three accumulators instead of only one, exactly the same constraints, number of intervals and initial conditions as before were used for the optimisation using the multiplexer. The objective function of the optimisation and the switching criterion were also the same.

The resulting profile of divider mass fraction and reflux ratio can be seen in fig. 8.1 and the results of the optimisation compared to the optimisation of the entire batch without the use of the multiplexer are summarised in tables 8.1 and 8.2.

As can be seen in the plot of the resulting profiles (fig. 8.1) the component C4 is not separated from the mixture during the off-cut but a large amount of component C4 ends up in the intermediate cut which is not desired during operation of the column. An additional constraint is necessary in order for the optimisation to be able to determine when the off-cut ends and the intermediate cut starts during periodic operation. Without such a constraint, there is no way of determining the optimal division of the two different cuts, and the optimisation problem becomes degenerate (i.e. it has an infinite number of solutions, all with exactly the same value of the objective function). From the simulation of the detailed model at base case (see fig 6.2) it can be observed that a constraint on the mass fraction of C4 to be less than 10% at the end of the off-cut, would be a good possibility to ensure that the appropriate switching conditions between off-cut and intermediate cut can be met. An optimisation with the

additional constraint should be performed, but because of time limitations it was not possible to include the optimisation in this thesis.

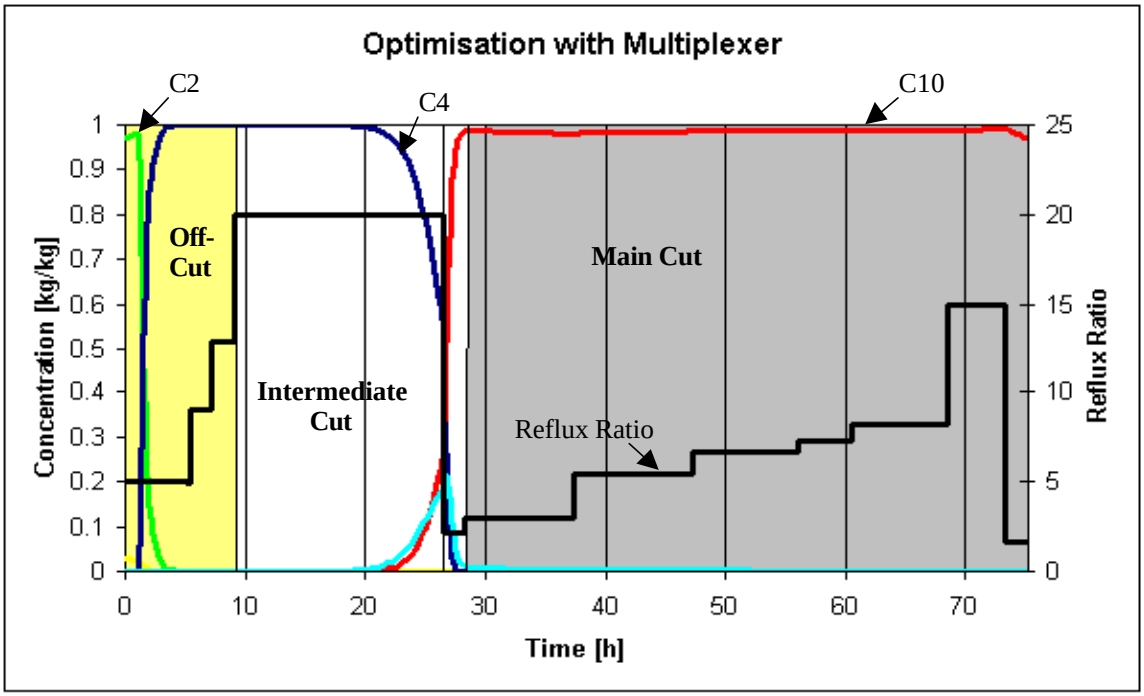

Figure 8.1 Reflux ratio and divider mass fraction profiles at optimum when using a multiplexer.

	Optimisation with multiplexer		Optimisation without multiplexer		Base case
Batch time	75 h	-15%	75 h	-15%	88 h
Product yield	5879 kg	+9.5%	5814 kg	+8.3%	5368 kg

Table 8.1 Results of the optimisation with multiplexer compared to base case.

	Optimisation with multiplexer	Optimisation without multiplexer
CPU time of optimisation	168472.6 sec (46.8 h)	147337 sec (40.9 h)
Number of optimisation iterations	78	85
Linear Algebraic Solver	MA28	MA28
Intervals of control variable optimised	13	13

Table 8.2 gPROMS performance during optimisation with multiplexer.

A more detailed summary of gOPT settings and gPROMS performance during the optimisations may be found in appendix D.

8.2 Optimisation of Periodic Operation

For the optimisation of periodic operation, new variables and parameters had to be introduced into the model. The holdup and the composition of the mixture in the reboiler at the beginning of every batch run was calculated as the mixture obtained by combining fresh feed with the contents of the intermediate cut accumulator at the end of the batch.

In order to perform a periodic optimisation the following additional equations were introduced into the accumulator model of the intermediate cut:

$$\Delta M_I(t) = M_I(t) - M_I^* \tag{8:1}$$

$$\Delta x_{I,i}(t) = x_{I,i}(t) - x_{I,i}^*(t) \tag{8:2}$$

Both M_I^* and $x_{I,i}^*$ are time-invariant parameters to be determined by the optimisation. They represent the amount of material and the mass fractions in the intermediate cut accumulator at the end of the batch. This interpretation can be implemented by enforcing the end-point constraint:

$$\Delta M_I(t_f)^2 + \sum_{i=1}^{10} \Delta x_{I,i}(t_f) \le e \tag{8:3}$$

which practically ensures that, at the final time t_f, $M_I(t_f) \approx M_I^*$ and $x_I i(t_f) \approx x_{Ii}^*$. Although theroretically ε should be set to 0, in practice a value of 10^{-6} was used to avoid an excessive number of optimisation iterations.

The material in the intermediate cut is recycled to the reboiler where it is mixed with the fresh feed. To account for this fact, the following variables and equations were introduced into the reboiler model:

$$\Delta M_B^* = M_F + M_I^* - M_B$$

$$\Delta x_{B,i}^* = \frac{M_F \cdot x_{F,i} + M_I^* \cdot x_{I,i}^*}{M_F + M_I^*} - x_{B,i}$$

where M_F and $x_{F,i}$ represent the amount and composition of the fresh feed respectively, while M_B and $x_{B,i}$ are the corresponding quantities for the combined feed. This allows us to impose the following initial conditions at the start of the optimisation:

$$\Delta M_B^*(0) = 0$$

$$\Delta x_{B,i}^*(0) = 0$$

which is equivalent to enforcing the desirable mixing constraints:

$$M_B(0) = M_F + M_I^*$$

$$(M_F + M_I^*) x_{B,i}(0) = M_F \cdot x_{F,i} + M_I^* \cdot x_{I,i}^*$$

As the light off-cut is not included explicitly in the model, its influence is approximated by the use of constants, λ_i:

$$\Delta M^{*}_{B,i}(0) = \left(M_{F,i} + M^{*}_{I,i}\right) \cdot l_i - M_{B,i}(0)$$

where λ_i is the fraction of component i removed during the light off-cut.

The objective function to be optimised was:

$$Profit = \left(\frac{M_{C10}}{t_{prod} + t_{setup} + t_{light\_off-cut}} \right) \tag{8:4}$$

where t_{setup} is approximated to 7 hours. $t_{light\_off\text{-}cut}$ was set to 7 hours as during the simulation.

An optimisation was performed with *fixed* amount and composition of the fresh feed. This optimisation resulted in a shorter production time, but less product was produced compared to the base case. The result is explained by the fact that the fresh feed was fixed during the optimisation. When the intermediate cut is optimised, the total feed charge will be less than before, because of less amount of mixture in the accumulator of the intermediate cut. This further means that less product will be obtained at the end of the next batch run. As a consequence the amount of product obtained during the intermediate cut will not be made smaller by the optimiser. Instead, only the time of production is decreased to maximise the objective function. However when the production time is decreased the yield of product during the main cut is not as large at the end of the operation as if the production time would be allowed to be longer, and this explains why the product yield obtained is actually less than during the base case. An easy way of getting around the problem is to optimise the amount of fresh feed as well. Thus an optimisation with the amount of fresh feed as an additional time invariant parameter was performed.

	Optimisation of periodic operation with fresh feed as fixed parameter		**Base Case**
Batch time	69 h	-22%	88 h
Product yield	5057 kg	-5.8%	5368 kg

Table 8.3 Results of optimisation of the periodic operation compared to base case.

8.3 Optimisation with Fresh Feed as Time Invariant Parameter

As predicted this optimisation resulted in both a decrease of production time and an improved yield of product. The production time was decreased by 10% and the yield of product was improved by 7.1% compared to the base case (see table 8.4). The results took 69 h for the gOPT solver to obtain. A detailed summary of the gOPT settings and the gPROMS performance during the optimisations may be found in appendix D. As can be seen in the plot of the resulting mass fraction and the reflux ratio profiles (see fig 8.2) the concentration of C4 clearly goes below 0.10, before the intermediate cut starts, to avoid too much of C4 in the charge to the next batch.

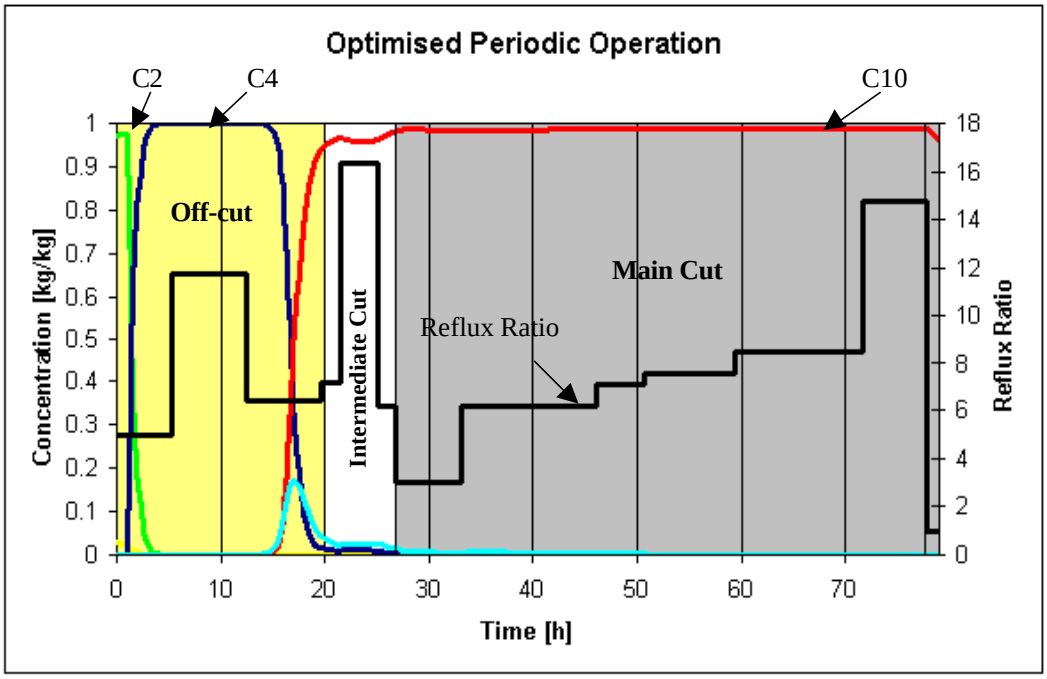

Figure 8.2 Reflux ratio and divider mass fraction profiles at optimum of the periodic operation.

	Optimisation of periodic operation with fresh feed as time invariant parameter		**Base Case**
Batch time	79 h	-10%	88 h
Product yield	5751 kg	+7.1%	5368 kg

Table 8.4 Results of optimisation of the periodic operation compared to base case.

A comparison of the reflux ratios of the optimisation with the multiplexer and the optimisation of the periodic operation also clearly shows that the reflux ratio profiles differ when there is an incentive to make the concentration of C4 lower during the intermediate cut. The difference makes the concentration of C10 in the intermediate cut accumulator at the periodic operation higher, as unwanted components are gathered in the off-cut accumulator instead.

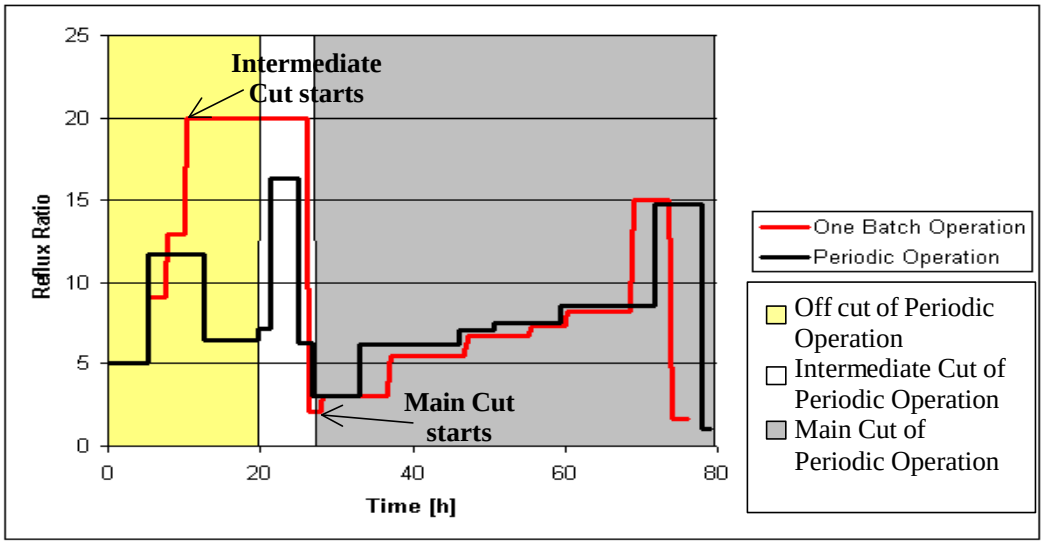

Figure 8.3 Comparison of the reflux ratios.

9. Conclusions and Directions for Future Work

9.1 Conclusions

The optimisation of the batch process shows that it is possible to reduce the time of production while simultaneously increasing the product yield, just by modifying the time variation of the reflux ratio. More specifically, results obtained from the performed optimisation of the model of the batch process were:

- 15% less time of production
- 9% higher product yield.

The optimisation took about 41 h of computation to perform on a SGI Origin 2000.

A new procedure of the reflux ratio could easily be realised in the plant without any additional investment costs and would result in a noticeable increase of profit.

However, as the actual process is operated periodically, the amount of product at the end of the operation is not the only factor that affects the profit. The mixture obtained during the intermediate cut that is mixed with the fresh feed also influences the production. This was accounted for when performing the optimisation of the periodic operation. The results from this optimisation were:

- 10.5% less time of production
- 7.9% higher product yield

The duration of the optimisation this time was about 69 h.

The results were obtained when the amount of fresh feed was considered as a degree of freedom for optimisation. If the fresh feed is set as a fixed parameter, i.e. not optimised during the whole periodic operation, the amount of product obtained will as a matter of fact be less than at base case.

An important conclusion to make regarding the performance of gPROMS is that it is possible to use gPROMS to optimise a detailed model of a batch distillation column within acceptable times of optimisation. However a very fast computer is needed, like for example a SGI Origin 2000 used in this work. The default solver in version 1.7 of gPROMS, MA48 was observed to not be as stable as the MA28 solver, which therefore was used in most cases, even though it requires slightly more computational time.

9.2 Directions for Future Work

In the immediate future the optimisation of the entire batch with the multiplexer formulation, including the additional constraint at the end of the off-cut, should be performed to make sure that reliable results are obtained.

The optimisation could include even more intervals, or the optimisation could be performed with just the number of intervals and a bound for the allowed time horizon of the whole operation time set, instead of fixing the number of intervals for each cut.

The model could be made even more detailed, for example by using tray efficiencies that vary over time. The time to simulate the model would then of course increase and it would be even more important to find a way to make the simulation of the model faster. One option could be to include equations used by the foreign object IKCAPE directly in the model. The solver of gPROMS would then work more effectively. A shorter simulation time would also make it possible to optimise the whole operation, including the light component off-cut and the heavy component off-cut making the optimisation results of the periodic operation more reliable.

The actual composition of the feed charged during one batch distillation can not be known precisely, as the composition of the fresh feed arriving from upstream units varies due to variations in process conditions. However the feed composition has shown to influence the operation procedure in a great extent (Gautheron [12]), thus optimisations with different feed compositions should be performed. This shows two potential areas for future work. First the optimisation of process operation under uncertainty due to the uncertain composition of the fresh feed, and secondly on-line optimisation to account for this uncertainty by improving operating conditions during the actual operation of each batch. However, the latter option requires a numerically tolerant model and very fast computing times during optimisation.

Finally, as already mentioned, the production is also performed with a packed column instead of a tray column. This batch process could also be optimised in *gPROMS* using the already, in SPEEDUP, developed model (see Gautheron [12]).

Nomenclature

A	Antoine's coefficient	
Area	cross sectional area	m^2
B	Antoine's coefficient	
bias	steady state control value	
C	Antoine's coefficient	
Cp	heat capacity	kJ/(kmol·K)
Error	set point and variable error	
f	fugacity	
F_{fak}	vapour load (F-factor)	$m/s \cdot (kg/m^3)^{0.5}$
g	acceleration due to gravity	m/s^2
gain	controller gain	
h	specific enthalpy	kJ/kmol
$\Delta H°_{298}$	latent heat of vaporisation	kJ/kmol
ΔHV^{298}	heat of vaporisation	kJ/kmol
height	liquid level in reflux drum	m
h_f	liquid level on tray	m
h_{weir}	weir height	m
h'_{weir}	height of liquid above weir	m
I_{error}	integral error	
I_{in}	input signal	
k	equilibrium coefficient	
k'	heat transfer coefficient	$W/m^2 \cdot K$
k_{liq}	liquid flow coefficient	$kmol \cdot m^{2/3}/h$
L	liquid flowrate	kmol/h
Level	liquid level in reboiler	m/m
l_w	weir length	m
M	molar holdup	kmol
MW	molecular weight	kmol/kg
N_C	number of components	
P	pressure	bar
p°	vapour pressure of pure component	Pa
ΔP	pressure drop	mbar
ΔP_{tr}	dry pressure drop	mbar
Q	rate of heat transfer	W
R	reflux ratio	
reset	reset time of PI-controller	
Sp	set point of PI-controller	
T	temperature	°C
U	internal energy	kJ
v	molar volume	$m^3/kmol$
$V_{downcomer}$	volume of downcomer	m^3
v_f	liquid load	$m^3/(m^2 \cdot h)$
value	calculated value of PI-controller	
Vges	volume reboiler	m^3
W	mass holdup	kg
w_g	vapour velocity	m/s
x	liquid composition	kmol/kmol
x_M	liquid composition	kg/kg
y	vapour composition	kmol/kmol

Greek Letters

ε_l	liquid fraction	
Φ	fugacity coefficient	
γ	activity coefficient	
η	tray efficiency	
λ	constant	
μ	parameter of control variable	
ρ	density	kg/m^3

Subscripts

B	batch
C	condenser
F	feed
I	intermediate cut
i	component
in	inlet
k	tray
out	outlet
R	reboiler drum
crit	critical point

Superscripts

L	liquid
V	vapour
*	ideal composition

References

[1] Barolo, M. and Fabrizio Berto, "Composition Control on Batch Distillation: Binary and Multicomponents Mixtures", *Ind. Eng. Chem. Res.*, **37**, 4689 (1998).

[2] Barolo, M. and F. Botteon, "Simple Method of Obtaining Pure Products by Batch Distillation", *AIChE J.*, **43**, 2601 (1997).

[3] Barolo, M., G.B. Guarise, N. Ribson, S. Rienzi, A. Trotta and S. Macchietto, "Some Issues in the Design and Operation of a Batch Distillation Column with a Middle Vessel", *Comput. Chem. Eng.* , **S20**, S37 (1996).

[4] Bosley, J.R. and Thomas F. Edgar, "An efficient dynamic model for batch distillation", *J. Proc. Cont.*, **4**, 195 (1994).

[5] Carlsson, E.C., "Don't Gamble With Physical Properties For Simulations", Chem. Eng. Progress (Oct 1996).

[6] Diwekar, U.M., "How Simple Can it be ? – A Look at the Models for Batch Distillation", *Comput. chem. Engng.*, **18**, S451 (1994).

[7] Diwekar, U.M., "Unified Approach to Solving Optimal Design Control Problems in Batch Distillation", *AIChE J.*, **38**, 1551 (1992).

[8] Diwekar, U.M., R.K. Malik and K. P. Madhavan, "Optimal Reflux Rate Policy Determination For Multicomponent Batch Distillation Columns", *Comput. Chem. Engng.*, **11**, 629 (1987).

[9] Furlonge, H.I., "*Optimal Operation of Unconventional Batch Distillation Columns*", PhD Thesis, University of London, January 2000.

[10] Furlonge, H.I., C.C. Pantelides and E. Sørensen, "Optimal Operation of Multivessel Batch Distillation Columns", AIChE J., **45**, 781 (1999).

[11] Galindez, H. and Å Fredenslund, "Simulation of Multicomponent Batch Distillation Processes", *Comput. Chem. Engng.*, **12**, 281 (1988).

[12] Gautheron, S., "*Modellierung und Optimierung von Batchdestillationskolonnen*", Diplomarbeit, Bayer AG Leverkusen (1999).

[13] Kooijman, H.A. and R. Taylor, "A Non-Equilibrium Model For Dynamic Simulation of Tray Distillation Columns", *AIChE J.*, **41**, 1852 (1995).

[14] Li, P., "*Entwicklung optimaler Führungsstrategien für Batch-Destillationsprocesse*", Doktorarbeit, Bayer AG Leverkusen (1998).

[15] Logsdon, J.S. and L.T. Biegler, "Accurate solution of differential-algebraic optimization problems", *Ind. Eng. Chem.*, **28**, 1628-1639 (1989).

[16] Nilsson, B., "*Föreläsningsanteckningar: Process Simulering*", Lund Institute of Technology, Lund (1999).

[17] Oh, M., *"Modelling and Simulation of Combined Lumped and Distributed Processes*", PhD Thesis, University of London (1995).

[18] Pantelides, C.C, *"Dynamic Behaviour of Process Systems"*, Lecture Notes, Centre for Process Systems Engineering, Imperial College of Science, Technology and Medicine, London (1998).

[19] Perry, R.H. and D. Green, "Perry's Chemical Engineers' Handbook, McGraw Hill Book Company, Inc New York, 6th ed., 1984.

[20] Process Systems Enterprise Ltd., *gPROMS Advanced User Guide*, London (1999).

[21] Process Systems Enterprise Ltd., *gPROMS Introductory User Guide*, London (1999).

[22] Sadotomo, H. and K. Miyahara, "Calculation procedure for multicomponent batch distillation", *Int. Chem. Engng.*, **23**, 56 (1983).

[23] Skogestad, S., B. Wittgens, E. Sørensen, and R. Litto, "Multivessel Batch Distillation", *AIChE J.*, **43**, 971 (1997).

[24] Vassiliadis, V.S., R.W.H. Sargent, and C.C. Pantelides, "Solution of a Class of Multistage Dynamic Optimisation Problems: 1. Problems without Path Constraints", *Ind. Eng. Chem. Res.*, **33**, 2111 (1994a).

[25] Vassiliadis, V.S., R.W.H. Sargent, and C.C. Pantelides, "Solution of a Class of Multistage Dynamic Optimisation Problems: 2. Problems with Path Constraints", *Ind. Eng. Chem. Res.*, **33**, 2123 (1994b).

Appendix A

Feed Composition

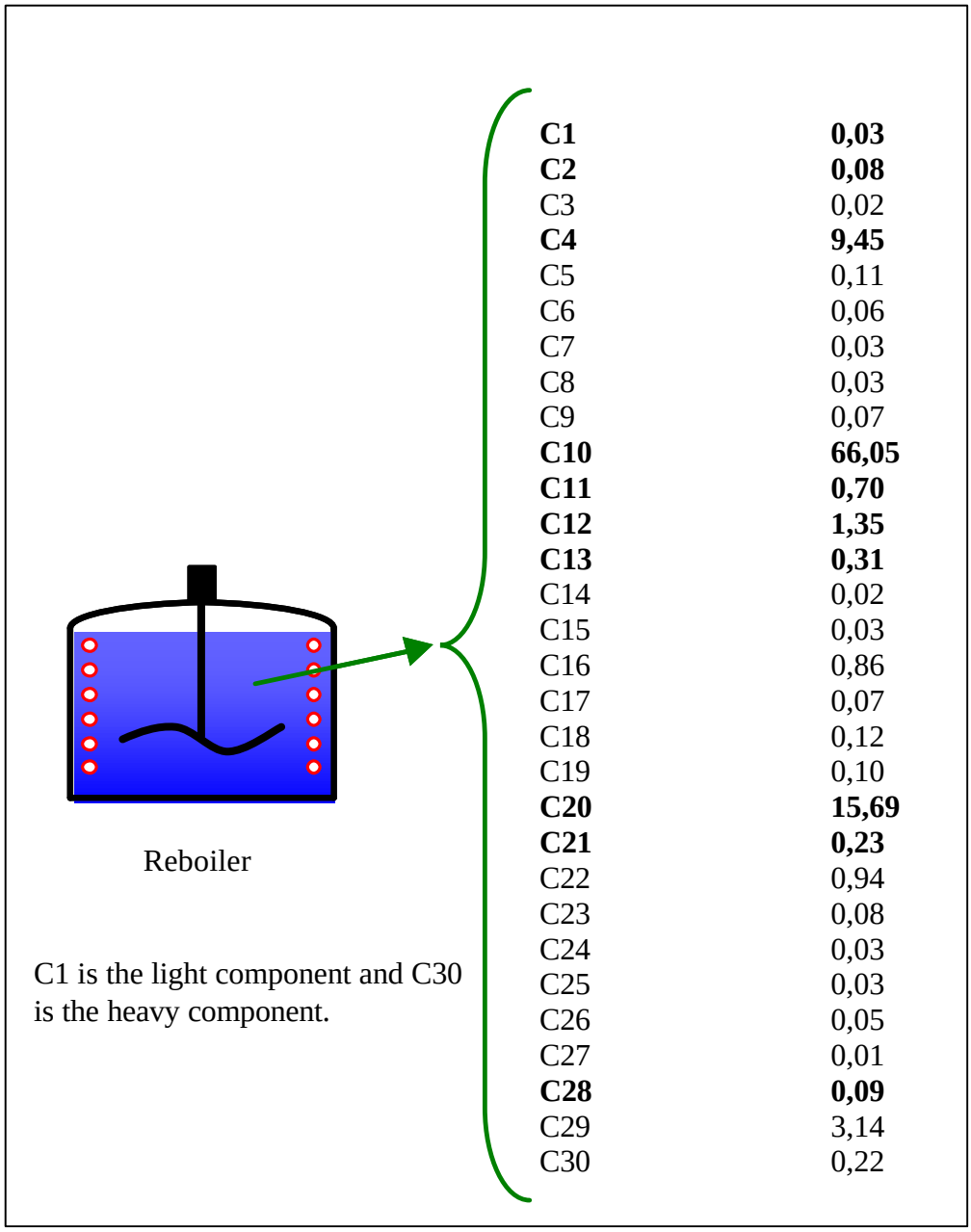

Figure A.1 GC analysis of the feed composition

Appendix B

The Equations of the Model

B.1 Tray

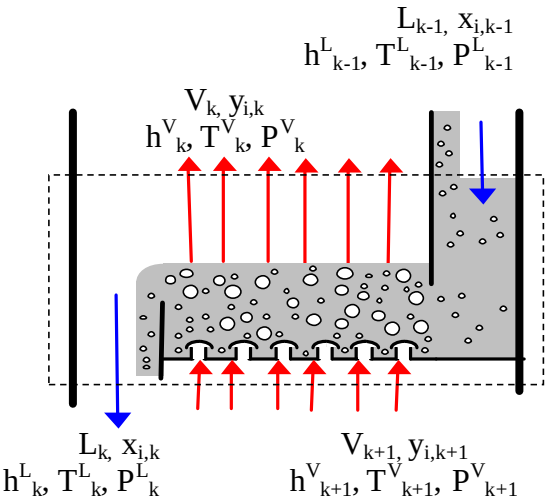

Figure B.1 Tray

Molar balance on component i:

$$\frac{dM_{i,k}}{dt} = x_{i,k-1} \cdot L_{k-1} + y_{i,k+1} \cdot V_{k+1} - x_{i,k} \cdot L_k - y_{i,k} \cdot V_k \qquad \text{i = 1,..N}_C \qquad \text{(B:1)}$$

Energy balance:

$$\frac{dU_k}{dt} = h^L_{k-1} \cdot L_{k-1} + h^V_{k+1} \cdot V_{k+1} - h^L_k \cdot L_k - h^V_k \cdot V_k \qquad \text{(B:2)}$$

Liquid and vapour contributions to component holdup:

$$M_{i,k} = x_{i,k} \cdot M^L_k + y_{i,k} \cdot M^V_k \qquad \text{i = 1,..N}_C \qquad \text{(B:3)}$$

Liquid and vapour contributions to total internal energy:

$$U_k = h^L_k \cdot M^L_k + h^V_k \cdot M^V_k - P_k \cdot v_k \qquad \text{(B:4)}$$

Equilibrium relationship:

$$y_{i,k} = h \cdot k_i \cdot x_i + (1-h) \cdot y_{i,k-1} \qquad \text{(B:5)}$$

Normalisation equations:

$$\sum_{i=1}^{N_C} x_{i,k} = \sum_{i=1}^{N_C} y_{i,k} = 1 \qquad \text{(B:6)}$$

Ideal mixing:

$$x_{i,k} = x_{i,k-1} \tag{B:7}$$

Liquid holdup on the tray:

$$M_k^L = \frac{(Area \cdot h'_{weir} \cdot e_l + V_{downcomer}) \cdot r_{liq}}{MW_{liq}} \tag{B:8}$$

Weir formula:

$$h'_{weir} = h_{weir} + \frac{1.45}{g^{1/3}} \cdot \left(\frac{L/l_w}{e_l} \right)^{2/3} + \frac{c}{2 \cdot g \cdot (r_{liq} - r_{vap})} \cdot \left(\frac{F_{Fak} - 0.2 \cdot \sqrt{r_{vap}}}{(1 - e_l)} \right)^2 \tag{B:9}$$

Liquid and vapour load:

$$v_f \cdot l_w \cdot r_{liq} = 10 \cdot L_k \cdot MW_{liq} \tag{B:10}$$

$$F_{Fak} = w_g \cdot r_{vap}^{1/2} \tag{B:11}$$

$$w_g \cdot r_{vap} \cdot Area = V_{k+1} \cdot MW_{vap} \tag{B:12}$$

Pressure drop across tray:

$$\Delta P = h_f \cdot r_{liq} \cdot g + \Delta P_{tr} \tag{B:13}$$

$$\Delta P_{tr} = f(F_{Fak}) \tag{B:14}$$

B.2 Reboiler Drum

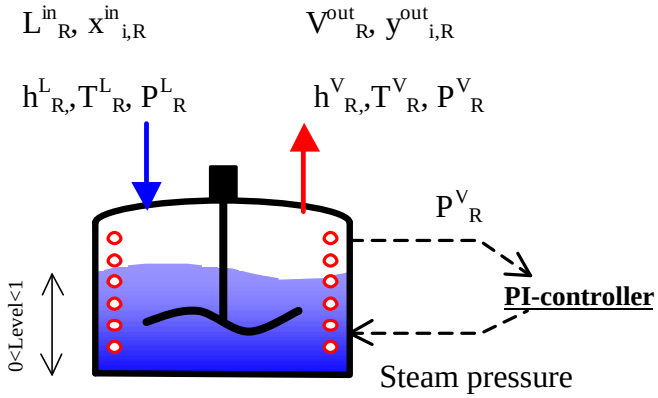

Figure B.2 Reboiler Drum

Molar balance on component i:

$$\frac{dM_{i,R}}{dt} = x_{i,R}^{in} \cdot L_R^{in} - y_{i,R}^{out} \cdot V_R^{out} \qquad \text{i = 1,..N}_C \tag{B:15}$$

Energy balance:

$$\frac{dU_R}{dt} = h_R^{in} \cdot L_R^{in} - h_R^V \cdot V_R^{out} + Q_R \tag{B:16}$$

Liquid and vapour contributions to component holdup:

$$M_{i,R} = x_{i,R} \cdot M_R^L + y_{i,R}^{out} \cdot M_R^V \qquad \text{i = 1,..N}_C \tag{B:17}$$

Equilibrium relationship:

$$y_i = k_i \cdot x_i \tag{B:18}$$

Normalisation equation:

$$\sum y_i = 1 \tag{B:19}$$

Liquid holdup:

$$Level \cdot V_{ges} \cdot r_{liq} = M \cdot MW_{liq} \tag{B:20}$$

Heat conduction:

$$Heat = 0.001 \cdot k' \cdot \left(A_{pipe} \cdot Level + A_{pipe,bottom}\right) \cdot \left(T_{steam} - T_{liq}\right) \tag{B:21}$$

$$T_{steam} = a \cdot \log\left(Steampressure\right) + b \tag{B:22}$$

where *a* and *b* are constants.

B.3 PI-controller

$$Error = Sp - I_{in} \tag{B:23}$$

$$\frac{d\left(I_{error}\right)}{dt} = Error \tag{B:24}$$

$$value = bias + gain \cdot \left(Error + \frac{I_{error}}{reset} \right) \tag{B:25}$$

B.4 Condenser

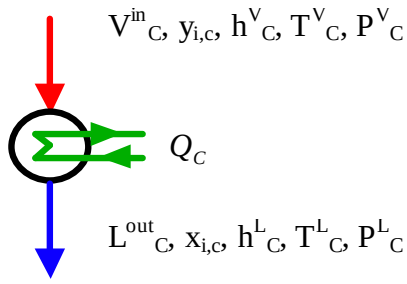

Figure B.3 Condenser

Molar balance on component i:

$$y_{i,c} = x_{i,c} \qquad i = 1,..N_C \qquad \text{(B:26)}$$

Molar balance:

$$V_C^{in} = L_C^{out} \qquad \text{(B:27)}$$

Energy balance:

$$h_1^V \cdot V_C^{in} = h_C^L \cdot L_C^{out} + Q_C \qquad \text{(B:28)}$$

Equilibrium relationship:

$$y_{i,out} = k_i \cdot x_{i,out} \qquad \text{(B:29)}$$

Normalisation equation:

$$\sum y_{i,out} = 1 \qquad \text{(B:30)}$$

B.5 Reflux Drum

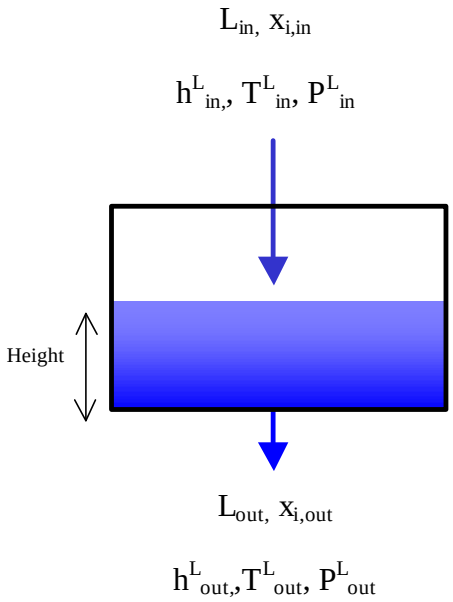

Figure B.4 Reflux Drum

Molar balance on component i:

$$\frac{dM_{i,k}}{dt} = x_{i,in} \cdot L_{in} - x_{i,out} \cdot L_{out} \qquad \text{i = 1,..N}_C \qquad \text{(B:31)}$$

Energy balance:

$$\frac{dU}{dt} = h_{in}^{L} \cdot L_{in} - h_{out}^{L} \cdot L_{out} \qquad \text{(B:32)}$$

Liquid holdup:

$$L_{out} = k_{liq} \cdot height^{1.5} \qquad \text{(B:33)}$$

$$M \cdot MW_{liq} = r_{liq} \cdot Area \cdot Height \qquad \text{(B:34)}$$

B.6 Divider

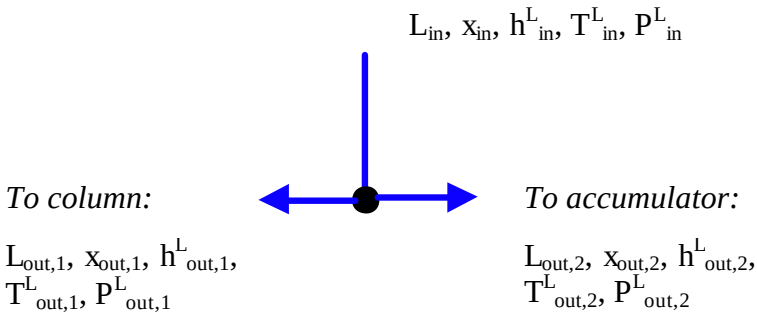

Figure B.5 Divider

Mass balance:

$$L_{in} = L_{out,1} + L_{out,2} \qquad \text{(B:35)}$$

$$L_{out,1} = L_{in} \cdot R \qquad \text{(B:36)}$$

Enthalpy balance:

$$h_{out,1}^{L} = h_{in}^{L} \cdot R \qquad \text{(B:37)}$$

$$h_{out,2}^{L} = h_{in}^{L} \cdot (1 - R) / R \qquad \text{(B:38)}$$

Equilibrium relationship:

$$x_{in} = x_{out,1} = x_{out,2} \qquad \text{(B:39)}$$

Pressure:

$$P_{in}^{L} = P_{out,1}^{L} = P_{out,2}^{L} \qquad \text{(B:40)}$$

Temperature:

$$T_{in}^{L} = T_{out,1}^{L} = T_{out,2}^{L} \qquad \text{(B:41)}$$

B.7 Accumulator

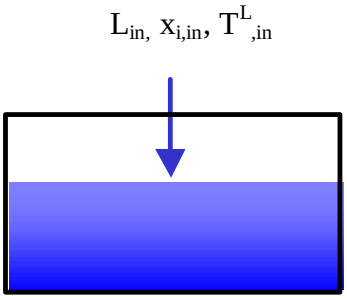

Figure B.6 Accumulator

Molar balance on component i:

$$\frac{dM_i}{dt} = x_{in,i} \cdot L_{in} \qquad \text{i = 1,..}N_C \qquad \text{(B:42)}$$

Liquid Volume:

$$Volume \cdot r_{liq} = M \cdot MW_{liq} \qquad \text{(B:43)}$$

Conversion to mass units:

$$W_i = MW_{liq,i} \cdot M_i \qquad \text{i = 1,..}N_C \qquad \text{(B:44)}$$

$$x_{M,i} = \frac{W_i}{\sum_{i=1}^{N_C} W_i} \qquad \text{(B:45)}$$

B.8 Equilibrium and Physical Properties Calculations

Equilibrium between the vapour and liquid phase is reached when the pressure, the temperature and the chemical potential of every component and the chemical potential of every component in both phases are the same. The equilibrium can be calculated by use of the fugacities, which will be equal in both phases at equilibrium:

$$f_i^{L} = f_i^{V}$$

This leads to:

$$g_i \cdot x_i \cdot f_i^{\circ} = \Phi_i \cdot y_i^{*} \cdot p$$

where the following approximations may be made:

- at low pressure: $f_i^{\circ} = p_i^{\circ}$
- ideal vapour phase: $\Phi_i = 1$
- ideal liquid phase: $g_i = 1$

The separation in most separation columns used in chemical industries are operated at relative low pressure and the vapour phase can therefore be assumed to be ideal. This leads to the expression:

$$k_i = \frac{y_i^{*}}{x_i} = \frac{p_i^{\circ}}{p} \cdot g_i$$

where the vapour pressure of every pure component, p_i° is calculated with the Antoine-equation:

$$\ln p_i^{\circ} = A_i + \frac{B_i}{C_i + T}$$

(the parameters A_i, B_i, C_i can be found in literature).

The activity coefficient, γ_i depends on both the temperature and concentration of the component and can be calculated with NRTL, UNIQUAC or UNIFAC models (Li [14])

Tray efficiency:

A theoretical tray means that vapour leaving the tray is in equilibrium with the liquid leaving the tray. In practice this never happens and tray efficiencies have to be used:

$$h_k = \frac{y_{i,k} - y_{i,k+1}}{y_{i,k}^{*} - y_{i,k+1}}$$

η_k is dependent of the volatility of the component and the efficiency of the mixing. η_k usually has a value between 0.7-1.0 and can easily be evaluated with an experiment. The tray efficiencies in this work have been assumed to be equal for all the components, although this is in reality only true for binary systems (Kooijman and Taylor [13]).

Capacity of the column:

The capacity of a separation column is often defined as the higher limit of the steam load. The steam load is limited by the diameter of the column, the tray structure and the characteristics of the mixture to be separated. If the steam load is too small the liquid will start leaking through perforations. This phenomenon is called *weeping*. If the steam load is too high on the other hand, it will cause the liquid to be entrained in the vapour up the column, causing *flooding*. The steam load effects the tray efficiencies in a great extent.

The load factor, F-factor is defined:

$$F_{Fak} = w_g \cdot r_{vap}^{1/2}$$

Enthalpy:

Enthalpies needed for the energy balances can be calculated with :

$$h_i^V = \Delta H^{\circ}_{298} + \int_{298}^{T} C_{p_i} dT$$

$$h_i^L = h_i^V - \Delta HV_i^{298}$$

The heat capacity, C_p and the heat of vaporisation depends on temperature and can be calculated with the following correlations:

$$C_{p_i} = a_{i,0} + a_{i,1} \cdot T + a_{i,2} \cdot T_j^2 + a_{i,3} \cdot T_j^3$$

$$\Delta HV_i = \Delta HV(T_i^v)\left(\frac{1 - T / T_{crit,i}}{1 - T_i^v / T_{crit,i}}\right)^{0.38}$$

The specific latent heat of vaporisation, ΔH°_{298} can be found in literature.

Appendix C

gOPT Settings and *gPROMS* Performance During Optimisation

	Off-cut & Intermediate cut	**Main cut**	**Entire batch**
CPU time of optimisation	11064 sec (3.1 h)	5056 sec (1.6 h)	147337 sec (40.9 h)
Number of optimisation iterations	13	13	85
Linear Algebraic Solver	MA28	MA48	MA28
Intervals of control variable optimised	6	7	13
Number of Linesearch Steps	13	14	113
Infeasible Linesearch Steps	0	0	5
CPU Time Spent on State Integration Only	2861 sec	1458 sec	43287 sec
CPU Time Spent on Sensitivity Integration Only	8201 sec	4146 sec	104035 sec
Mean (Sensitivity+State)/State CPU Ratio	4.1	4.3	4.2
Optimisation tolerance	10^{-4}	10^{-4}	10^{-4}
Absolute integration tolerance	10^{-6}	10^{-6}	10^{-6}
Relative integration tolerance	10^{-6}	10^{-6}	10^{-6}
Steady State tolerance	10^{-6}	10^{-6}	10^{-6}
Event location tolerance	10^{-9}	10^{-9}	10^{-9}

Table C.1 gOPT settings and gPROMS performance during optimisations.

Appendix D

gOPT Settings and *gPROMS* Performance During Optimisation of Periodic Operation

	Optimisation with multiplexer	**Optimisation with fresh feed as time invariant parameter**
CPU time of optimisation	168472.6 sec (46.8 h)	247746.3 sec (68.8 h)
Number of optimisation iterations	78	86
Linear Algebraic Solver	MA28	MA28
Intervals of control variable optimised	13	13
Number of Linesearch Steps	97	159
Infeasible Linesearch Steps	4	7
CPU Time Spent on State Integration Only	35804	59085
CPU Time Spent on Sensitivity Integration Only	132650	188629
Mean (Sensitivity+State)/State CPU Ratio	5.7	7.0
Optimisation tolerance	10^{-4}	10^{-4}
Absolute integration tolerance	10^{-6}	10^{-6}
Relative integration tolerance	10^{-6}	10^{-6}
Steady State tolerance	10^{-6}	10^{-6}
Event location tolerance	10^{-9}	10^{-9}

Table D.1 gOPT settings and gPROMS performance during optimisations.